mathematics

MDPI

Article

Efficient Red Kite Optimization Algorithm for Integrating the Renewable Sources and Electric Vehicle Fast Charging Stations in Radial Distribution Networks

Sami M. Alshareef * and Ahmed Fathy *

Department of Electrical Engineering, College of Engineering, Jouf University, Sakaka 72388, Saudi Arabia
* Correspondence: smalshareef@ju.edu.sa (S.M.A.); afali@zu.edu.eg (A.F.)

Abstract: The high penetration of renewable energy resources' (RESs) and electric vehicles' (EVs) demands to power systems can stress the network reliability due to their stochastic natures. This can reduce the power quality in addition to increasing the network power losses and voltage deviations. This problem can be solved by allocating RESs and EV fast charging stations (FCSs) in suitable locations on the grid. So, this paper proposes a new approach using the red kite optimization algorithm (ROA) for integrating RESs and FCSs to the distribution network through identifying their best sizes and locations. The fitness functions considered in this work are: reducing the network loss and minimizing the voltage violation for 24 h. Moreover, a new version of the multi-objective red kite optimization algorithm (MOROA) is proposed to achieve both considered fitness functions. The study is performed on two standard distribution networks of IEEE-33 bus and IEEE-69 bus. The proposed ROA is compared to dung beetle optimizer (DBO), African vultures optimization algorithm (AVOA), bald eagle search (BES) algorithm, bonobo optimizer (BO), grey wolf optimizer (GWO), multi-objective multi-verse optimizer (MOMVO), multi-objective grey wolf optimizer (MOGWO), and multi-objective artificial hummingbird algorithm (MOAHA). For the IEEE-33 bus network, the proposed ROA succeeded in reducing the power loss and voltage deviation by 58.24% and 90.47%, respectively, while in the IEEE-69 bus it minimized the power loss and voltage deviation by 68.39% and 93.22%, respectively. The fetched results proved the competence and robustness of the proposed ROA in solving the problem of integrating RESs and FCSs to the electrical networks.

Keywords: electric vehicles; charging stations; renewable energy; red kite optimization algorithm

MSC: 90C31

Citation: Alshareef, S.M.; Fathy, A. Efficient Red Kite Optimization Algorithm for Integrating the Renewable Sources and Electric Vehicle Fast Charging Stations in Radial Distribution Networks. *Mathematics* **2023**, *11*, 3305. https://doi.org/10.3390/math11153305

Academic Editor: Ioannis G. Tsoulos

Received: 12 June 2023
Revised: 20 July 2023
Accepted: 24 July 2023
Published: 27 July 2023
Corrected: 24 July 2024

1. Introduction

Recently, there has been a rapid growth in the use of fossil fuel sources, especially in electric power generation plants and the transportation sector. These sources increase environmental pollution as they emit greenhouse gas; they also cause global warming [1]. Therefore, many countries are looking to replace gasoline vehicles with clean energy cars, known as electric vehicles (EVs), to reduce the amount of pollution [2]. EVs are environmentally friendly, but have different economic costs than gasoline ones. EVs have advanced batteries and power electronic devices that enable them to be installed to grids as controllable loads. The integration of EVs to power systems faces great challenges like violation of transmission line thermal constraints due to overload; this may cause a voltage drop in some sensitive buses. Also, the uncertainties associated with these vehicles represent challenges to: the distribution network operator, as the sources of uncertainties are time rounding; the amount of daily energy consumption; the range of driving; and the EV battery capacity [3]. When EVs charge from public charging stations, mostly fast charging stations (FCSs) are utilized by demanding high power from the grid to reduce the required charging duration to meet the required battery state-of-charge (SOC). However,

the high demand required by these stations causes negative effects on the distribution network, as they increase the network power losses and voltage deviations. However, to reduce the demand on the grid, renewable energy sources (RESs) can be installed to supply the excess loads during peak time. Identifying the optimal allocations of RESs and FCSs in the distribution network is mandatory to minimize their associated negative effects. Improvement of the power generation from RESs is essential; various technologies have been presented to improve the power quality of renewable energy sources integrated in the microgrid [4,5].

Many reported approaches have been implemented to identify the best allocations and sizes on both RESs and FCSs. Amer et al. [6] presented a planning model to evaluate the sizes and sites of FCSs in addition to wind turbines in distribution networks. The authors considered the stochastic features of RESs, FCSs, and residential EV loads. In [7], parking lots and capacitor allocations have been identified in the electrical distribution network via a biogeography-based optimizer (BBO) to compensate the system reactive power. A multi-objective problem was introduced and solved via hybrid and grey wolf optimizers (GWO) and the particle swarm optimizer (PSO) to allocate FCSs, and shunt capacitors and distributed generators (DGs) [8]. Reducing the cost of power loss, minimizing the voltage fluctuation, reducing the development costs of FCSs, minimizing the costs of EV energy consumption, and reducing the costs of DGs have been considered as targets. Bayram et al. [9] determined the allocations of parking lots via a combinatorial optimization algorithm and the two-stages stochastic programming model. A comprehensive review of allocating the EV rapid charging stations based on economic benefits has been conducted by Gupta et al. [10]. A planning method for penetrating FCSs in the electrical distribution network has been presented in [11] to find the optimal operators, traffic conditions, vehicles, power grids, and drivers. Moreover, the authors used real-time data for the practical third ring of Beijing. In [12], the non-dominated sorting genetic algorithm II (NSGA-II) was presented to evaluate the places and sizes of FCSs and DGs installed in the electrical distribution network. The considered targets are mitigating the EV user loss, minimizing the power loss, reducing the cost of FCS development, and enhancing the voltage shape. A FCS connected to the grid has been simulated in [13] such that the harmonic currents were minimized. Moreover, an energy management strategy has been presented via integrating the photovoltaic (PV) generation system. Pal et al. [14] identified the best allocations of FCSs and solar DGs in addition to battery storage system in the electrical distribution network using the hybrid Harris hawks optimizer and GWO. The targets are mitigating the energy loss, investment costs, operating and maintenance costs, and the voltage violation index. Moreover, the number of charging ports, FCSs' capacities, and the captured power via EVs have been evaluated. A planning model of FCS has been introduced and solved by binary PSO to minimize the costs of construction, operating and maintenance, trips to the station, and power loss [15]. In [16], optimal places and capacities of FCSs and RESs integrated to the distribution network have been identified when considering the uncertainties of renewable-based generators. Also, the capacitated deviation flow refueling location-based model has been presented to cover the EVs' charging demands on transportation network. Amer et al. [17] developed a stochastic program to evaluate the optimal locations and sizes of small wind turbines connected to FCSs in urban and suburban areas. Moreover, a worthiness metric has been employed to classify the FCS candidate sites according to the EV drivers' attractiveness. The EV charging station place was evaluated in the electrical network and covered by the transportation network using HHO and differential evolution (DE) [18]. The targets are mitigating the voltage fluctuation, minimizing the energy loss, and reducing the cost of land for maximizing the service to EV with minimized founding costs. A quantum-behaved Gaussian mutational dragonfly algorithm (QGDA) has been employed to conduct the best planning of capacitors and EV charging stations in the distribution network [19]. The authors in [20] reviewed various configurations of charging station designs, and the different modes of renewable DGs were summarized. Ahmad et al. [21] solved the problem of sitting solar-operated charging stations integrated to the grid using

an improved chicken swarm optimizer where the network voltage profile was enhanced while the power loss and operating cost were minimized. Moreover, the authors used a stochastic method to forecast the EV demand and the neural network to predict the power generated from the solar PV plant. The places of charging stations integrated to the grid have been evaluated via the hybrid metaheuristic approach comprising the chicken swarm optimizer (CSO) and the teaching learning-based optimizer (TLBO) [22]. A solar hybrid EV charging station has been presented to mitigate the dependence on the main grid [23]. The authors used a stochastic model to forecast the EV arrival time, battery SOC, and charging demand. Moreover, a stochastic firefly algorithm (SFA) has been used as a maximum power point tracker (MPPT) for the solar system to extract its maximum power. Furthermore, SFA has been employed to solve multi-objective planning to mitigate the investment cost and enhance the charging profit. In [24], the sizing problem of EV charging stations has been solved via optimization frameworks to reduce the charging station investment cost and provide a certain quality of service to the client. The locations of FCSs in the distribution network have been identified via solving multi-objective problems using a transient search optimizer (TSO) to mitigate the active and reactive losses and enhance the network voltage stability [25]. A model with two stages for optimizing charging stations and charging schedules has been presented by Yi et al. [26] to achieve complete satisfaction among members of society. The load demand and starting point of the trip have been predicted via Monte Carlo simulations in the first phase while a binary PSO has been employed in the second one to find the optimal path of the trip. In [27], the state-of-the-art features for many design approaches of FCSs have been reviewed in addition to the future challenges of each one. Zhou et al. [28] presented a model to calculate the charging station's total operating cost which is divided into economic and environmental costs. Also, the locations of these stations in Irish regions have been identified using a genetic algorithm (GA) where the total cost is reduced. A black widow optimizer (BWO) has been used to identify the optimal places of charging stations and renewable DGs in the distribution system with the aid of model predictive control (MPC) that simulates the actual SOC of storage batteries [29]. Many methods conducted in optimizing the charging station have been reviewed and categorized according to the fitness functions, algorithms, constraints, modeling of EV uncertainties, and DG integration [30]. In [31], FCSs, solar PV, and storage batteries have been installed in distribution networks with sizes and locations decided by hybrid NSGA-II and Fuzzy satisfaction. The authors considered many targets, like system power loss, voltage violation, flow of served EVs, costs of investment, operation and maintenance of PV, and charging stations. The planning of charging station location and battery-swapping stations have been presented as multi-objective problems to mitigate the total cost, enhance the satisfaction of user, and reduce the EV's consumed energy [32]. A hybrid approach combining the student psychology optimizer and the AdaBoost algorithm has been introduced to allocate the EV charging station linked to distribution generation such that the peak power and voltage regulation are mitigated [33]. Al Wahedi et al. [34] implemented a techno-economic analysis via the HOMER software for renewable-based charging stations to evaluate its optimal configuration in different cities in Qatar. Excessive review of different nature-inspired optimizers employed in solving the problem of FCS placement has been presented in [35]. The optimal planning of FCSs has been expressed as a multi-objective problem with multi-criteria decision-making [36]. Minimizing the total charging time and cost is the main target of the work presented in [37] to model the vehicle charging via a bi-level optimizer. The optimal locations of EV parking lots in smart distribution systems have been identified using a hybrid metaheuristic algorithm to reduce the network loss and voltage fluctuation [38]. Moreover, the cost of EV charging/discharging and the cost of purchased power from the grid are considered in the presented problem. Fathy et al. [39] presented a competition over resource (COR) approach to determine the optimal sites and sizes of EV parking lots in the electrical distribution system. The authors considered the cost of reliability enhancement, investment cost, and the cost of power loss improvement as the targets to be minimized. Table 1 outlines most

of the reported methods to integrate RESs and FCSs in electrical networks, the reader can observe the following items:

- Most of the reported works used metaheuristic optimization algorithms to integrate RESs and FCSs to the network.
- Many of these methods lack accuracy due to the fall in local optimal solution in addition to the slow convergence rate of some approaches.
- Also, the reported hybrid algorithms were complicated to implement and required excessive effort and time.
- Many researchers ignored the installation of distributed generators (DGs) and they relied mainly on the grid as the source of energy.

The authors considered all these shortages in the reported methods and covered them via the following contributions:

- A new methodology incorporating the simple and efficient red kite optimization algorithm (ROA) is proposed to evaluate the optimal capacities and places of RESs and FCSs in distribution networks.
- The considered fitness functions are: reducing the network active loss and minimizing the voltage deviation.
- A multi-objective red kite optimization algorithm (MOROA) is proposed to reduce both targets.
- The proposed approach competency is proved through the obtained results.

The paper is outlined as follows: Section 2 explains the model of th considered system; the form of the optimization problem is presented in Section 3; the basics of ROA are introduced in Section 4; the proposed ROA-based methodology is explained in Section 5; the results and discussions are presented in Section 6; and Section 7 handles the conclusions.

Table 1. Outlines of most reported methods to integrate the RESs and FCSs in electrical networks.

Author	Year	DG	Type	Objective	Algorithm	Metaheuristic	Remarks
Amer et al. [6]	2020	√	wind	- Maximize the revenues of both wind DGs and FCS. - Minimize the total associated costs.	Genetic algorithm	√	The genetic algorithm has a slow convergence rate
Sachan et al. [7]	2020	×	--	- Minimize total losses.	Biogeography-based optimizer	√	The installation of DGs is ignored
Mohanty et al. [8]	2022	√	NA	- Minimize the cost of power loss. - Minimize the voltage violations. - Minimize the EV energy consumption cost. - Minimize the cost of DGs.	GWO-PSO	√	The presented hybrid algorithm is complicated and requires excessive effort for implementation
Zeng et al. [9]	2020	√	wind	Maximize the overall profit of parking lots	Genetic algorithm	√	The genetic algorithm has a slow convergence rate
Kong et al. [11]	2019	√	NA	Minimize the costs of construction and operation	Iterative optimization algorithm	×	The authors considered fast charging stations for all EVs
Battapothula et al. [12]	2019	√	NA	- Minimize the EV user loss - Minimize the power loss - Minimize the cost of FCS development - Enhance the network voltage profile	NSGA-II	√	NSGA-II is very complicated in construction and implementation
Khan et al. [13]	2019	√	PV	Minimize the net power exchange between the charging station and grid	Constant current-constant voltage	×	An energy management strategy between DG, charging station, and grid has been implemented

Table 1. *Cont.*

Author	Year	DG	Type	Objective	Algorithm	Metaheuristic	Remarks
Pal et al. [14]	2021	√	Solar	- Minimize the energy loss - Minimize voltage violations - Minimize investment, operation, and maintenance costs	Harris hawks optimizer and GWO	√	Both HHO and GWO are easy to trap in local optima
Wu et al. [15]	2021	×	--	- Minimize the costs of construction, operation, and maintenance - Minimize the EV travel cost - Minimize the power loss cost	Binary PSO	√	PSO can not avoid the local optima and has a low convergence rate
aSa'adati et al. [16]	2021	√	Wind and solar	Minimize the costs of investment and energy losses	CFRLM	×	The authors ignored the driving range uncertainty and the EV's SOC during arrival at the transportation network
Amer et al. [17]	2021	√	wind	- Maximizing the FCS and DG profits gained from FCSs - Minimize the network energy losses	Genetic algorithm	√	The genetic algorithm has a slow convergence rate
Pal et al. [18]	2021	×	--	- Minimize of the energy loss - Minimize the voltage violation - Minimize the land cost	DE and HHO	√	The authors ignored the installation of DGs
Rajesh et al. [19]	2021	√	NA	- Minimize the total losses - Minimize the network voltage violation	Quantum-behaved Gaussian mutational dragonfly algorithm	√	The employed approach is difficult and requires large computational time

Table 1. *Cont.*

Author	Year	DG	Type	Objective	Algorithm	Metaheuristic	Remarks
Ahmad et al. [21]	2021	√	Solar	- Improve the voltage profile - Mitigate the power loss	Improved chicken swarm optimizer	√	Many steps are followed in the presented approach that make it complicated in implementation
Deb et al. [22]	2021	×	--	Minimize the overall cost of FSC construction	CSO-TLBO	√	The optimal sites of swapping stations and EV charging have not been considered
Goswami et al. [23]	2021	√	Solar	- Minimize the investment cost - Maximize the charging station profit	Stochastic firefly algorithm	√	Firefly suffers from high complexity, computational time, and slow convergence speed
Khaksari et al. [24]	2021	×	--	Minimize the investment cost of FCS	Gurobi optimization	×	Gurobi optimization is limited to the complexity of the handled problem. Also, it is not fast enough to solve complex problems
Bhadoriya et al. [25]	2022	√	NA	Mitigate the total active power loss	Transient search optimizer	√	TDO may trap in local optima during handling complex problems with high dimensions
Yi et al. [26]	2022	×	--	Minimize the annual cost paid by the car owners and investors	Binary PSO	√	PSO falls in local optima and has a slow convergence rate
Zhou et al. [28]	2022	×	--	Minimize the total social cost	Genetic algorithm	√	The genetic algorithm has a slow convergence rate
Aljehane et al. [29]	2022	√	RESs	Reduce the charging time and cost	Black widow optimizer	√	BWO can not avoid the local optima and has a slow rate of convergence
Kumar et al. [31]	2022	×	--	Mitigate the investment cost, power loss, and voltage deviation	Fuzzy optimized via NSGA-II	√	NSGA-II is very complicated in construction and implementation

Table 1. *Cont.*

Author	Year	DG	Type	Objective	Algorithm	Metaheuristic	Remarks
Zu et al. [32]	2022	×	--	- Reduce the total cost - Enhance the user satisfaction - Mitigate the EV's consumed energy	CPLEX and YALMIP languages	×	The solver needs high memory for solving complex problems
Thangaraju [33]	2022	√	NA	Minimize the annualized costs	Student psychology optimizer and AdaBoost algorithm	√	Large consumed time is required for implementing the student psychology optimizer
Al Wahedi et al. [34]	2022	√	Wind and PV	Minimize investment and operating costs	HOMER	×	Detailed inputs, data, and time are mandatory to obtain adequate results from HOMER
Erdogan et al. [36]	2021	×	--	Minimize the overall cost of charging station	Multi-objective optimization (MOO)	NA	The presented MOO method is not clear, also the authors did not consider DG installation
Ma et al. [37]	2021	×	--	Minimize the daily charging time	Surrogate optimization algorithm	√	The surrogate optimization algorithm has a slow convergence rate
Ahmadi et al. [38]	2021	√	Wind and PV	Minimize the loss and voltage fluctuation	- Genetic PSO - Genetic imperialist competitive algorithm (GICA)	√	Excessive computational time is required by both employed hybrid approaches
Fathy et al. [39]	2020	×	--	- Enhance the network reliability - Reduce the investment cost - Minimize the cost of power loss	Competition over resource	√	The authors did not consider the installation of DGs

2. The Considered System Model

The integration of renewable-based DGs and EVs in the distribution network is considered in this work. This section presents the models of the photovoltaic (PV) system, wind turbines (WT), and electric vehicles (EVs).

2.1. Model of the PV System

The PV system transforms light to electrical energy, and has many methods employed in producing electrical energy from sunlight irradiance. It composes a series of cells to produce the required voltage. The generation of the PV system relies on temperature and solar radiation striking its surface, so it is essential to consider both terms while studying the PV system's behavior. Normal operating cell temperature (NOCT) is used as an indicator of cell temperature that can be computed as follows [40]:

$$T_c = T_a + \frac{NOCT - 20^\circ}{0.8} \cdot G \tag{1}$$

where T_a is ambient temperature and G is irradiance.

The cell generated power can be expressed as

$$P_c = P \times [\eta \times (T_c - 25^\circ)] \tag{2}$$

where P is the cell rated power and η is the efficiency of the solar cell. The PV panel generated power can be obtained via multiplying the cell output power by the number of cells as follows:

$$P_{Panel} = n_{cell} \times P_c \tag{3}$$

where n_{cell} denotes the number of cells in the panel. The used temperature and solar radiation daily profiles are shown in Figure 1 [41].

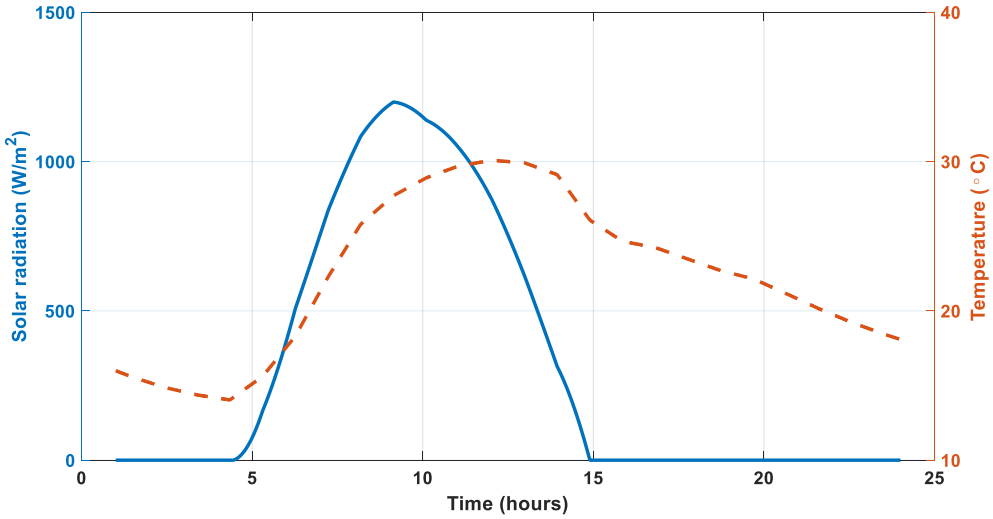

Figure 1. Daily profiles of temperature and solar radiation.

2.2. Model of a Wind Turbine

The wind turbine (WT) output power depends on the wind speed and wind direction in addition to the geography site of installation and wind density. The extracted power from WT can be written as follows:

$$P_{WT}(t) = \begin{cases} 0 & V < V_{cut-in} \text{ or } V > V_{cut-off} \\ P^r_{WT}\left(\frac{P_{WT0}-P^r_{WT}}{V_{cut-off}-V_r}\right)(V(t)-V_r) & V_r < V \leq V_{cut-off} \\ P^r_{WT}\left(\frac{V(t)-V_{cut-in}}{V_r-V_{cut-in}}\right)^3 & V_{cut-in} \leq V \leq V_{cut-off} \end{cases} \quad (4)$$

where P^r_{WT} is the WT rated power, V_{cut-in}, V_r, and $V_{cut-off}$ are the cut-in, rated, and cut-off speeds of the turbine, respectively, V is wind speed, and P_{WT0} is WT power at the cut-off speed. The WT output power can be calculated as [42]

$$P_{Wind-total} = n_{WT} \times P_{WT} \quad (5)$$

where n_{WT} denotes wind turbine number. The wind speed daily profile is given in Figure 2 [41].

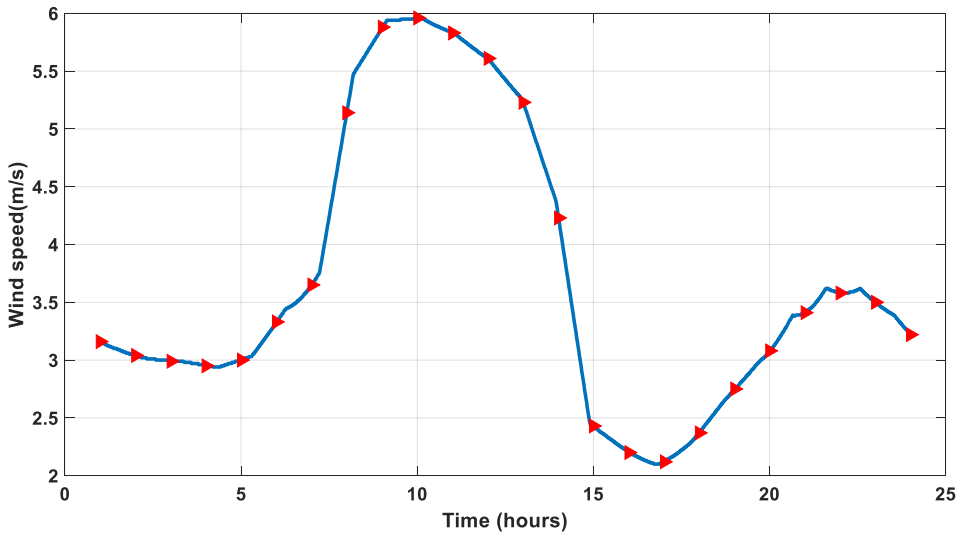

Figure 2. Wind speed daily profile.

2.3. Model of an Electric Vehicle

In order to model the EVs, three elements should be considered which are the expected mileage per day, the consumed energy per mile, and the wait time spent in the station. The first one can be simulated through lognormal distribution [43]; the lognormal distribution probability density function (PDF) can be computed as

$$f(x) = \frac{1}{\sqrt{2\pi}\sigma x} exp\left(-\frac{(ln(x)-\mu)^2}{2\sigma^2}\right), \; x > 0 \quad (6)$$

where x is a random number with one variance and zero mean, μ and σ denote the location and scaling parameters, respectively, and they can be calculated as follows:

$$\mu = ln\left(\frac{m}{\sqrt{1+\frac{v}{m^2}}}\right), \; \sigma = \sqrt{ln\left(1+\frac{v}{m^2}\right)} \quad (7)$$

where m and v represent the standard deviation and mean created via historical data. The expected mileage per day can be expressed as follows:

$$M_d = e^{(\mu_m + \sigma_m \times \sqrt{-2 \times lnc_1} \times cos(2\pi c_2))} \quad (8)$$

where σ_m and μ_m are the parameters of lognormal probability distribution, respectively, and c_1 and c_2 are random variables that follow the normal distribution; they are in the range of [0, 1]. The values of σ_m and μ_m can be calculated with the aid of the standard deviation (σ_{md}) and mean (μ_{md}) of EV mileage statistical data as follows:

$$\mu_m = ln\left(\frac{\mu_{md}^2}{\sqrt{\mu_{md}^2 + \sigma_{md}^2}}\right), \sigma_m = \sqrt{ln\left(1 + \frac{\sigma_{md}^2}{\mu_{md}^2}\right)} \tag{9}$$

The second important parameter that should be considered while modeling the EV is the consumed energy per mile, it can be computed as [44]

$$E_m = \alpha \times K_{EV}^b \tag{10}$$

where α and b represent the EV model constant coefficients and K_{EV} is the total energy supplied via battery. The EV can travel the maximum mileage (M_{dMax}) with a fully charged battery through the following formula:

$$M_{dMax} = \frac{B_{Cap}}{E_m} \tag{11}$$

where B_{Cap} is the battery capacity, and the charging demand can be computed as follows:

$$E_d = \begin{cases} B_{Cap} & M_d \geq M_{dMax} \\ M_d \times E_m & M_d < M_{dMax} \end{cases} \tag{12}$$

A Gaussian distribution can be used to calculate the waiting time spent in the station as follows [45]:

$$t_a = \mu_a + \sigma_a \cdot x_1, t_d = \mu_d + \sigma_d \cdot x_2 \tag{13}$$

$$t_{dur} = t_d - t_a \tag{14}$$

where t_a, t_d, and t_{dur} are arrival, departure, and charging duration times, respectively, σ_a, σ_d, μ_a, μ_d are standard deviations and means of entrance/leaving of EV to/from the station, and x_1 and x_2 are random numbers with one variance and zero mean.

The required state of charge ($SOC^{desired}$) of EV battery can be calculated as follows [44]:

$$SOC^{desired} = min\left\{\left(SOC^{init} + \frac{E_d}{B_{Cap}}\right), \left(SOC^{init} + \frac{t_{dur}}{B_{Cap}} \cdot r_{ch}\right)\right\} \tag{15}$$

where SOC^{init} and r_{ch} are the battery's initial state of charge and charging rate, respectively. In this study, four EVs with specifications given in Table 2 are considered [44]. The layout of the considered model is shown in Figure 3.

Table 2. The specifications of the four considered EVs.

Vehicle Model	Honda Accord	Toyota Prius	Chevrolet Volt	Ford Fusion
Consumed power	29 kW/mile	29 kW/mile	36 kW/mile	34 kW/mile
Distance with battery capacity	13 miles	11 miles	37 miles	21 miles
Capacity of battery	6.6 kWh	4.4 kWh	16 kWh	7.6 kWh
Maximum rate of charge	6.6 kW	3.5 kW	3.5 kW	3.5 kW

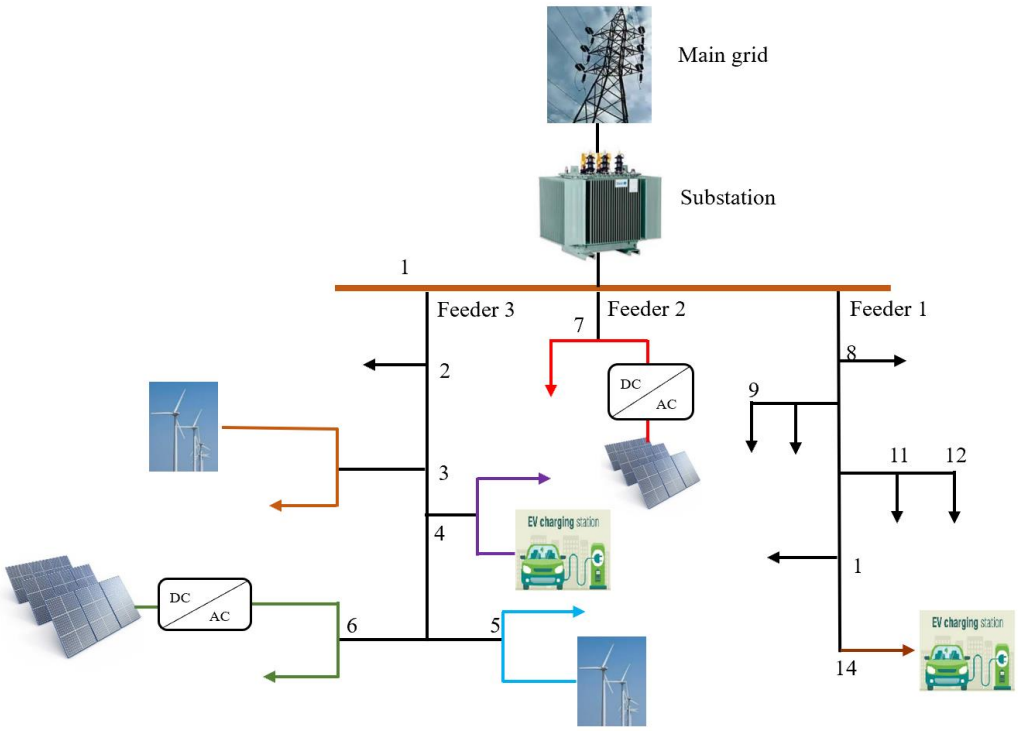

Figure 3. Layout of the considered model.

3. Form of Optimization Problem

In this section, the objective function and constraints are established to allocate and seize the renewable energy DGs and EV charging stations. Minimizing the total power loss of the network and reducing the voltage violation are the two considered objective functions. The accompanied constraints are supply-demand balance, limits of bus voltage, thermal constraint, generation limits, and constraints related to EVs.

3.1. Network Power Loss

The active power loss of the network is considered as the first target, it can be written as follows:

$$f_1 = Minimize\ P_{loss} \tag{16}$$

$$P_{loss} = \sum_{t=1}^{24} \sum_{i=1}^{n_b} \sum_{j>1}^{n_b} Y_{ij} \left(V_{i,t}^2 + V_{j,t}^2 + 2V_{i,t}V_{j,t}cos\left(\delta_{i,t} - \delta_{j,t}\right) \right) \tag{17}$$

where n_b is the number of branches, $V_{i,t}$ and $V_{j,t}$ are the magnitudes of voltage at buses i and j during time t, respectively, $\delta_{i,t}$ and $\delta_{j,t}$ are the voltages' angles at buses i and j, respectively, and Y_{ij} is the admittance of feeder $i-j$. The mitigation of the network losses is the required target from the distribution system operator perspective.

3.2. Network Voltage Violation

The second target is reducing the network voltage violation; the penetrations of RESs and FCSs to the grid may increase the capacity of supply part, this helps in reducing the losses and enhancing the voltage violation. This can be expressed as follows:

$$f_2 = Minimize \sum_{t=1}^{24} \sum_{i=1}^{n_b} |1 - V_{i,t}| \tag{18}$$

3.3. Constraints

Balance of supply-demand, limits of bus voltage, thermal limits, generation limits, and constraints related to EVs are five constraints considered in the formulated problem.

3.3.1. Supply-Demand Balance

This constraint is given by load flow analysis, the supplied power at each bus should be equal to the demand power plus the power losses of the branches connected to this bus. This can be written as follows:

$$P_{gi,t} - P_{di,t} = P_{chi,t} + |V_{i,t}| \sum_{j=1}^{n_b} |Y_{ij}||V_{j,t}| cos(\delta_{i,t} - \delta_{j,t} - \theta_{ij}) \quad (19)$$

$$Q_{gi,t} - Q_{di,t} = |V_{i,t}| \sum_{j=1}^{n_b} |Y_{ij}||V_{j,t}| sin(\delta_{i,t} - \delta_{j,t} - \theta_{ij}) \quad (20)$$

where $P_{gi,t}$, $P_{di,t}$, and $P_{chi,t}$ are the generated, demand, and EV charged active powers at bus i during time t, respectively, $Q_{gi,t}$ and $Q_{di,t}$ are the generated and demand reactive powers at bus i during time t, respectively, and θ_{ij} is the angle of Y_{ij}.

3.3.2. Bus Voltage Constraint

During integrating charging station and RESs, the bus voltage should be kept inside its normal limits as follows:

$$V^{min} \leq V_{i,t} \leq V^{min} \quad (21)$$

$$\delta^{min} \leq \delta_{i,t} \leq \delta^{min} \quad (22)$$

where *min* and *max* denote minimum and maximum values.

3.3.3. Thermal Constraint

Integrating the EV to the grid increases the transmission line power flow, therefore the temperature of lines will raise, the power flow should not exceed the allowable range, this can be written as follows:

$$|S_{i,t}| \leq |{S_i}^{max}|, \; i = 1, \; 2, \ldots, \; n_b \quad (23)$$

where $S_{i,t}$ is the power flow in line i at time t while ${S_i}^{max}$ is the maximum allowable flow in line i.

3.3.4. Generation Limit

The generated power from renewable energy DGs should be in its normal limits as follows:

$${P_{RES}}^{min} \leq P_{RESi,t} \leq {P_{RES}}^{max} \quad (24)$$

where $P_{RESi,t}$ is the output power from RES installed at bus i during time t, and ${P_{RES}}^{min}$ and ${P_{RES}}^{max}$ denote the minimum and maximum generated powers from RES, respectively.

3.3.5. EV Constraint

The power required by the EV should be inside *min* and *max* limits as follows:

$${P_{EV}}^{min} \leq P_{EVi,t} \leq {P_{EV}}^{max} \quad (25)$$

where $P_{EVi,t}$ is the output power from EV connected to bus i at time t, and ${P_{EV}}^{min}$ and ${P_{EV}}^{max}$ represent the minimum and maximum required powers by EV, respectively.

4. The Basics of the Red Kite Optimization Algorithm

The red kite optimization algorithm (ROA) is a novel metaheuristic approach introduced by Gahruei et al. [46]; it was inspired by the red kites' social life. The red kites usually build nests near lakes and wooded areas that are suitable for hunting. They live together, with random movements, and are affected by each other's positions during flight, and they use high speed while hunting. They have voices, called the sound of unity, that have been generated in times like finding good bait, water source, migration, and birth. Also, the sounds that occur in times of danger such as enemy attack, death of another animal, earthquake, and storm are known as the sound of danger. To simulate the behavior of a

red kite in finding food, each bird can be defined through its position, value of evaluation function, amount of displacement of points, sound of danger (in the direction of the individual component), sound of unity (in the direction of the social component), new position of the bird, and new evaluation function. In order to obtain good results, the metaheuristic algorithm must first navigate the problem search space well to prevent trapping in local optima. Then it gradually moves from the exploration to exploitation phase and exploits the best solution in the last iterations. ROA has three main stages which are explained as follows:

1. **The first stage—the initial position of the birds:** In this stage, according to Equation (26), the position of red kites can be initialized randomly as,

$$Pos_{i,j}(t) = lb + rand \times (ub - lb),\ i = 1,\ 2, \ldots, n\ and\ j = 1, 2, \ldots, d \tag{26}$$

where $Pos_{i,j}(t)$ is i^{th} red kite's position at iteration t, lb and ub are lower and upper boundaries, respectively, n is size of population, d denotes problem dimension, and $rand$ is a random number in [0, 1].

2. **The second stage—selection of the leader:** Selecting the leader is obtained according to Equation (27):

$$\overrightarrow{Best(t)} = \overrightarrow{Pos_i(t)}\ if\ f_i(t) < f_{best}(t) \tag{27}$$

where $Best(t)$ denotes position of the best bird in iteration t, $Pos_i(t)$ denotes the position of i^{th} red kite in iteration t, $f_i(t)$ is value of the bird evaluation function in iteration t, and $f_{best}(t)$ is the value of the evaluation function of the best bird in iteration t.

3. **The third stage—the movement of the birds:** It is considered that red kites must gradually move from exploration phase to exploitation stage through considering decreasing coefficient (D) according to Equation (28).

$$D = \left(exp\left(\frac{t}{t\_max} \right) - \frac{t}{t\_max} \right)^{-10} \tag{28}$$

where t is the current iteration and t_max denotes the maximum iteration.

The birds update their positions through Equations (29) and (30):

$$\overrightarrow{pos_i^{new}(t+1)} = \overrightarrow{Pos_i(t)} + \overrightarrow{P_{mi}(t+1)} \tag{29}$$

$$\overrightarrow{P_{mi}(t+1)} = D(t) \times \overrightarrow{P_{mi}(t)} + \overrightarrow{SC(t)} \odot \left(\overrightarrow{Pos_{rws}(t)} - \overrightarrow{Pos_i(t)} \right) + \overrightarrow{UC(t)} \odot \left(\overrightarrow{Best(t)} - \overrightarrow{Pos_i(t)} \right) \tag{30}$$

where $Pos_{rws}(t)$ is the bird position selected by roulette wheel in iteration t, $pos_i^{new}(t+1)$ denotes the new position of the bird, and SC and UC are random vectors of social and individual components, respectively. After updating the position, it is important to check the search space boundaries, this can be conducted using Equation (31) as,

$$\overrightarrow{pos_i^{new}(t+1)} = max\left(min\left(\overrightarrow{pos_i^{new}(t+1)} + ub \right), lb \right) \tag{31}$$

The new temporary position will be replaced if the evaluation function is improved. In such case, $Pos_i(t+1)$ is equal to $pos_i^{new}(t+1)$. As mentioned, SC and UC are random vectors of social and individual components, they represent the voice of unity and danger of each bird, and they are obtained according to the following relation:

$$\begin{cases} \overrightarrow{SC(t+1)} = \vec{r_1} \\ \overrightarrow{UC(t+1)} = \vec{r_2} \end{cases} if\ rand \leq 0.5$$

$$\begin{cases} \overrightarrow{SC(t+1)} = \vec{r_3} \\ \overrightarrow{UC(t+1)} = \vec{r_1} \end{cases} Otherwise \quad (32)$$

where $\vec{r_1}$ is a random vector in [1, 2], $\vec{r_2}$ is a random vector in [1, 3], and $\vec{r_3}$ is a random vector in [0, 1].

In the ROA, based on the current position of each bird, the position of a neighbor is randomly chosen via a roulette wheel and the best solution found so far. In the early iterations, the value of $D(t)$ is close to one for exploring and searching new spaces. In the movement based on the individual component, the red kite explores new spaces based on its position and that of a randomly selected neighbor. The social component also leads the algorithm to global optimum. Gradually, as the algorithm moves from the initial iterations to intermediate iterations, the coefficient $D(t)$ decreases to achieve balance between the exploration and exploitation phases. In the final iterations, this coefficient tends to zero and the algorithm exploits searching for the best solution among the obtained good solutions. The ROA is characterized by its ease in structure and execution, also it has few controlling parameters and a high convergence rate. The flowchart of the ROA is shown in Figure 4.

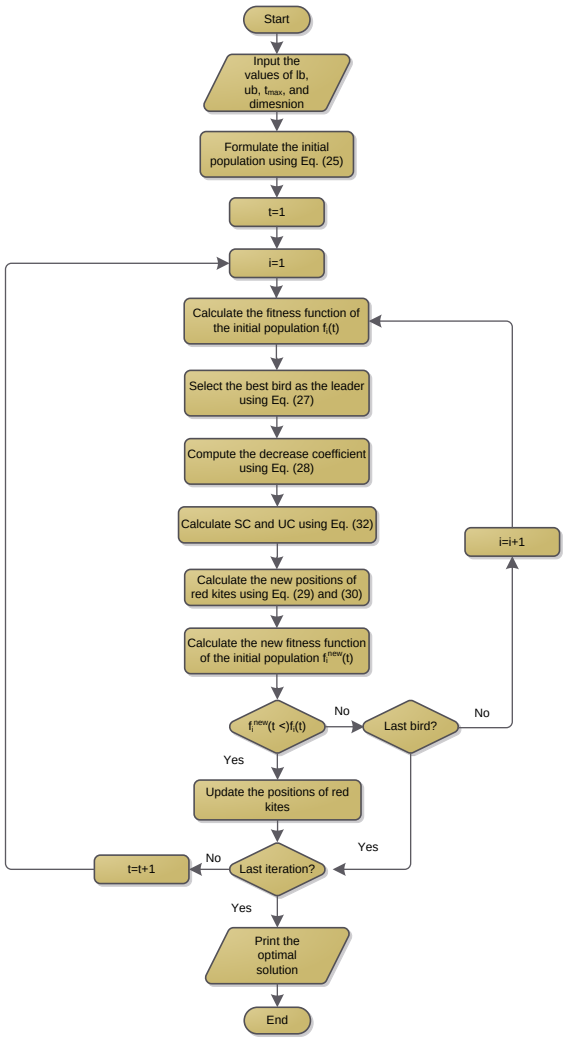

Figure 4. ROA flowchart.

5. The Proposed ROA-Based Methodology

This work proposes a new approach of the ROA to identify the optimal sites and sizes of RESs and FCSs in a radial distribution network. The considered objective functions are selected based on the distributor operator's point of view, and are mitigating the network power loss and minimizing the voltage fluctuation. Also, a new multi-objective ROA is proposed to achieve both targets. The assigned memory of the problem is divided into four vectors that represent the locations and sizes of RESs and FCSs as shown in Figure 5. The process of updating followed in the ROA using Equations (29) and (30) is adapted such that the first and third vectors of the variables have integer numbers assigned to the best sites of both RESs and FCSs. The most key features that characterize the proposed ROA are simplicity of the construction, need of few controlling parameters, and balance between exploration and exploitation phases. These features enhance the convergence rate of the algorithm and prevent falling in local optima. All these merits encourage the authors to apply the ROA in solving the presented problem. The proposed ROA pseudo code assigned to solve the single objective problem is given in Algorithm 1.

Algorithm 1 The proposed ROA pseudo code to solve the single objective optimization problem.

1: Define the ROA parameters like max iteration (*t_max*), size of population (*n*), *d*, *lb*, *ub*, and number of runs (*n_run*).
2: Input the load data and line data of the network under study.
3: Conduct load flow analysis and keep the voltage fluctuation and power loss.
4: Formulate the initial population using Equation (26).
5: for $i = 1$: n
6: Integrate Pos_i in the network, where Pos_i is the probable solution from the population.
7: Conduct power flow for the network with integrating Pos_i.
8: Compute the initial evaluation function $(f_i(Pos_i))$.
9: end for
10: while $k > n\_run$ do
11: for $t > t\_max$ do
12: for $i = 1$: n
13: Calculate the values of *SC*, *UC*, and *D* using Equations (28) and (32).
14: Calculate the red kites' new positions using Equations (19) and (30).
15: Check the positions' limits using Equation (31).
16: Compute the new objective function $(f_i^t(pos_i^{new})$.
17: if $f_i^t(pos_i^{new}) > (f_i^{t-1}(Pos_i)$
18: Update Pos_i bu pos_i^{new}
19: end if
20: $i = i + 1$
21: end for
22: $t = t + 1$
23: end for
24: end for
25: $k = k + 1$
26: end while
27: Save the optimal places and sizes of RESs and FCSs.

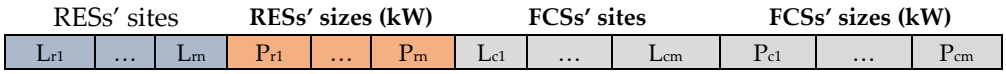

Figure 5. The proposed ROA memory.

A multi-objective red kite optimization algorithm (MOROA) is proposed to minimize both power loss and voltage violation, two components of archiving and hunting the food are proposed in MOROA. The first one saves the nondominant solutions achieved so far while the other component selects the best one from the obtained archive. Moreover, the solution entrance to the archive is controlled via considering the archive controller.

When the new solution is governed by one archived solution, it should be excluded from the archive entering. On the other hand, if the new solution is governed via one or more archived solutions, it will be included in the archive and the governed solutions are ignored. Also, when recent solutions and archive members have no control between them, it must be included in the archive. The top solution is chosen from the archive using the roulette wheel method as follows:

$$P_i = \frac{C}{N_i} \tag{33}$$

where C is a constant with a value greater than unity and N_i is the number of pareto solutions.

6. Numerical Analysis and Discussions

The analysis was performed on two standard distribution systems, which are the IEEE-33 bus network and the IEEE-69 bus network; the proposed ROA was simulated for 100 iterations, 50 population sizes, and 10 independent runs [47]. The maximum generation of RESs (PV and WT) was 1000 kW, and 1500 kW for FCS [44]. Three cases were studied in each network, the first one was minimizing power loss whereas the second one was mitigating network voltage fluctuation. The last case was a multi-objective to reduce both power loss and voltage fluctuation.

6.1. IEEE-33 Bus Network

The network single line diagram is shown in Figure 6; the network had 32 branches and 33 nodes, its nominal voltage was 12.66 kV while 100 MVA was the base power. In this network, it was assumed that two RESs were required to be installed, the first one was PV and the second one was WT. Also, two FCSs were integrated to the network to serve 200 vehicles selected randomly from Table 2 over 24 h. The base loads were 3.715 MW and 2.3 MVar while the network losses were 3905.628 kW and 2604.031 kVar. Figure 7 shows the demand level as a percentage of the base demand during each hour. The proposed ROA was implemented, and the fetched results were compared to other approaches of the dung beetle optimizer (DBO) [48], the African vultures optimization algorithm (AVOA) [49], the bald eagle search (BES) algorithm [50], the bonobo optimizer (BO) [51], and the grey wolf optimizer (GWO) [52] which are programmed. The analysis was performed using a laptop with specifications of 11th Gen Intel(R) Core(TM) i7-11370 @3.30 GHz processor, and 16.00 GB RAM.

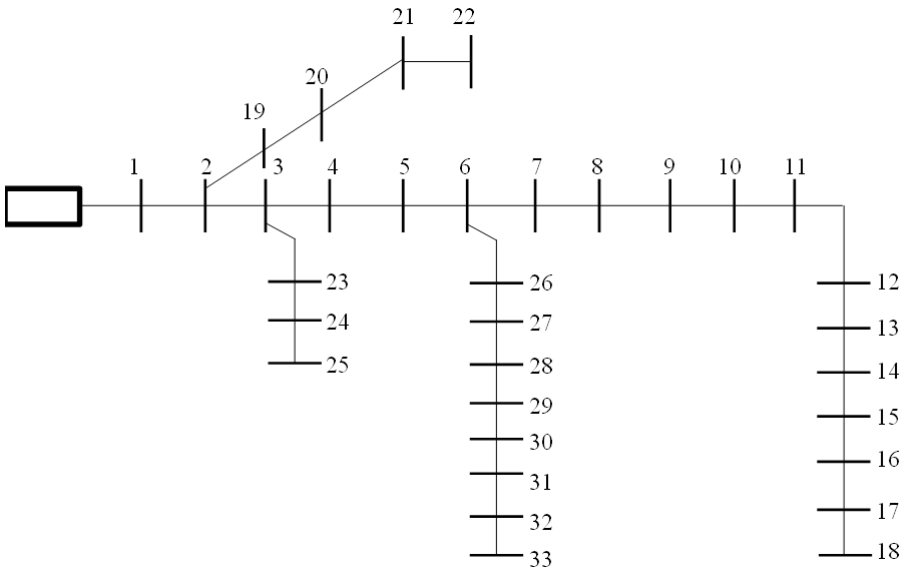

Figure 6. IEEE-33 bus network single line diagram.

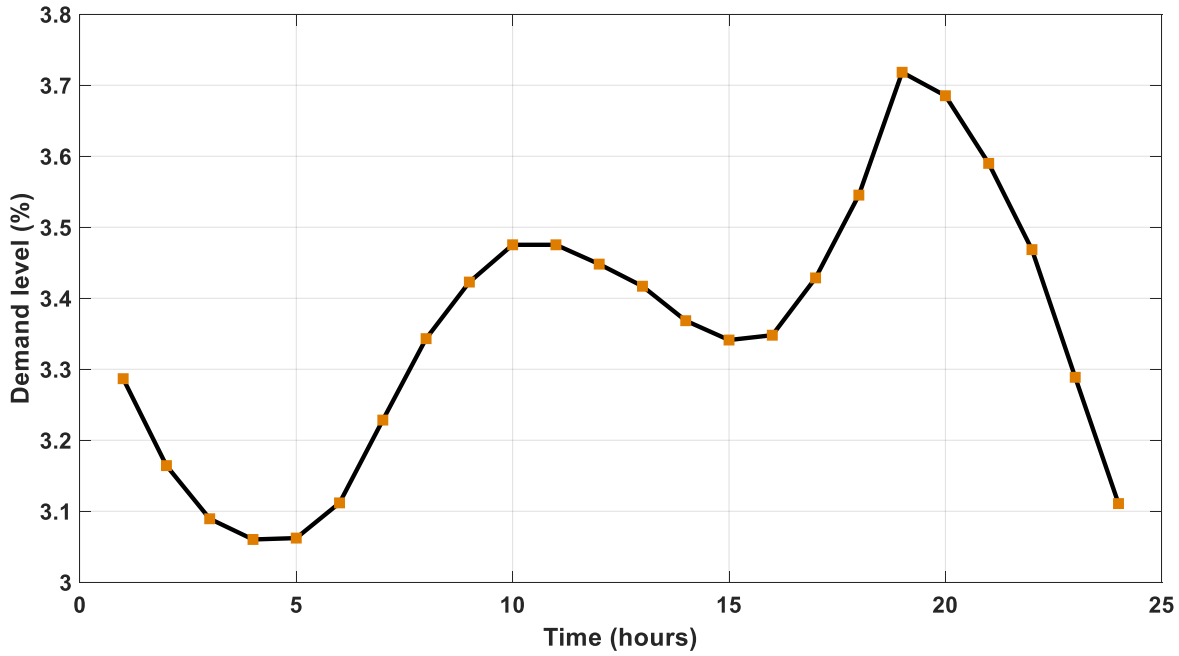

Figure 7. The daily load demand of the IEEE-33 bus network.

The fetched results during minimizing the power loss are given in Table 3. The proposed ROA achieved the best power loss over 24 h with a value of 1631.1189 kW obtained with integrating a RES of 770.3162 kW and 1126.969 kW on buses 13 and 30, respectively, and a FCS of 63.34486 kW and 50.23074 kW on buses 30 and 2, respectively. In such case, the voltage violation of the network was 14.5663 pu. On the other hand, BO came second with a power loss of 1633.4916 kW through integrating RESs and FCSs of 1072.105 kW, 870.675 kW, 103.400 kW, and 103.950 kW on buses 30, 13, 2, and 13, respectively. The highest power loss was 1716.946 kW, obtained via AVOA. The results proved the preference of the proposed ROA in such case. Another important item that is considered in comparison is the computational time required to implement one run, it is clear that the proposed ROA is the fastest one as it consumed 64.569 s., whereas the slowest one is BES with 131.489 s. The power loss versus number of iterations is shown in Figure 8. The voltage profiles of the network throughout minimizing the power loss are shown in Figure 9. The proposed ROA achieved good improvement in the voltage profile, being better than the original network.

Table 3. The optimal results throughout minimizing the first objective function of the IEEE-33 bus network.

	DBO	**AVOA**	**BES**	**BO**	**GWO**	**ROA**
RES (kW)/location	1172.455/(30) 768.3386/(13)	1415.316/(8) 841.6776/(30)	767.7161/(13) 1073.831/(30)	1072.105/(30) 870.675/(13)	796.258/(13) 1179.83/(30)	770.3162/(13) 1126.969/(30)
FCS (kW)/location	99.000/(33) 107.05/(2)	109.800/(26) 107.625/(19)	104.8500/(2) 112.6125/(19)	103.400/(2) 103.950/(13)	79.4101/(6) 95.9678/(30)	63.34486/(30) 50.23074/(2)
Active power loss (kW)	1650.078	1716.946	1641.0623	1633.4916	1652.1002	1631.1189
Reactive power loss (kVar)	1067.1	1104.5	1060.6	1067.3	956.48116	947.36830
Vmin (pu)/location	0.9718/(33)	0.9609/(18)	0.9724/(33)	0.9692/(18)	0.9707/(33)	0.9708/(33)
Vmax (pu)/location	1.000/(1)	1.000/(1)	1.000/(1)	1.000/(1)	1.000/(1)	1.000/(1)
Voltage deviation (pu)	14.1639	15.2245	14.2351	15.2438	14.5806	14.5663
Time (s)	92.287	89.6085	247.461	66.547	131.489	64.569

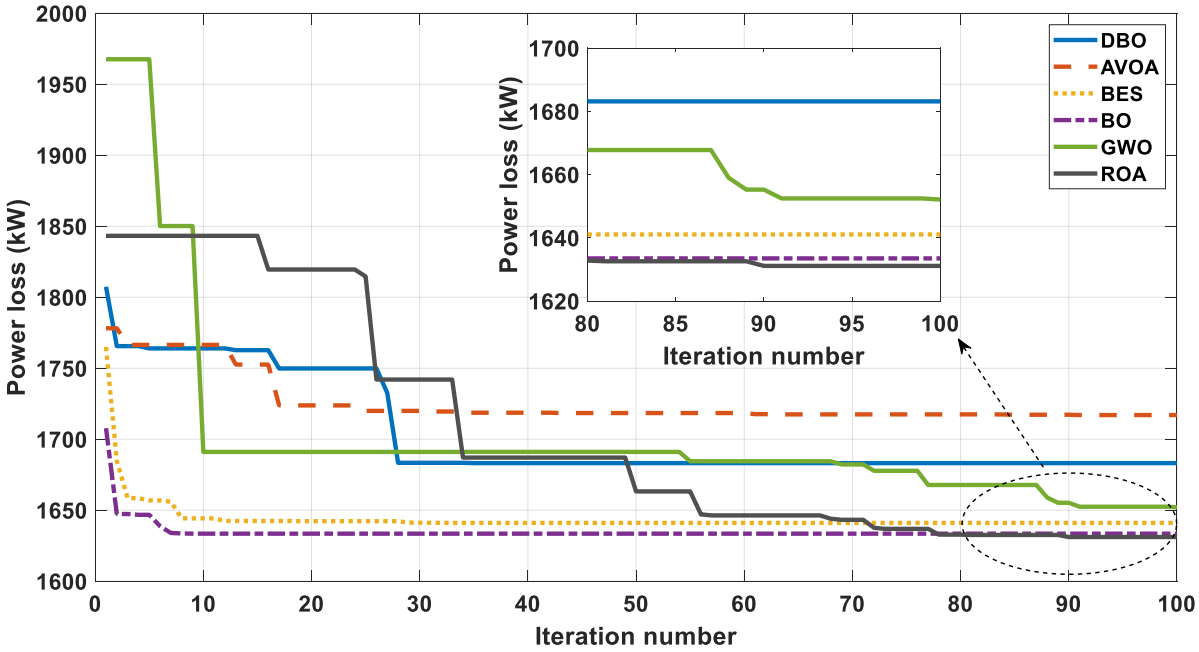

Figure 8. Power loss variation throughout minimizing the first objective function of the IEEE-33 network.

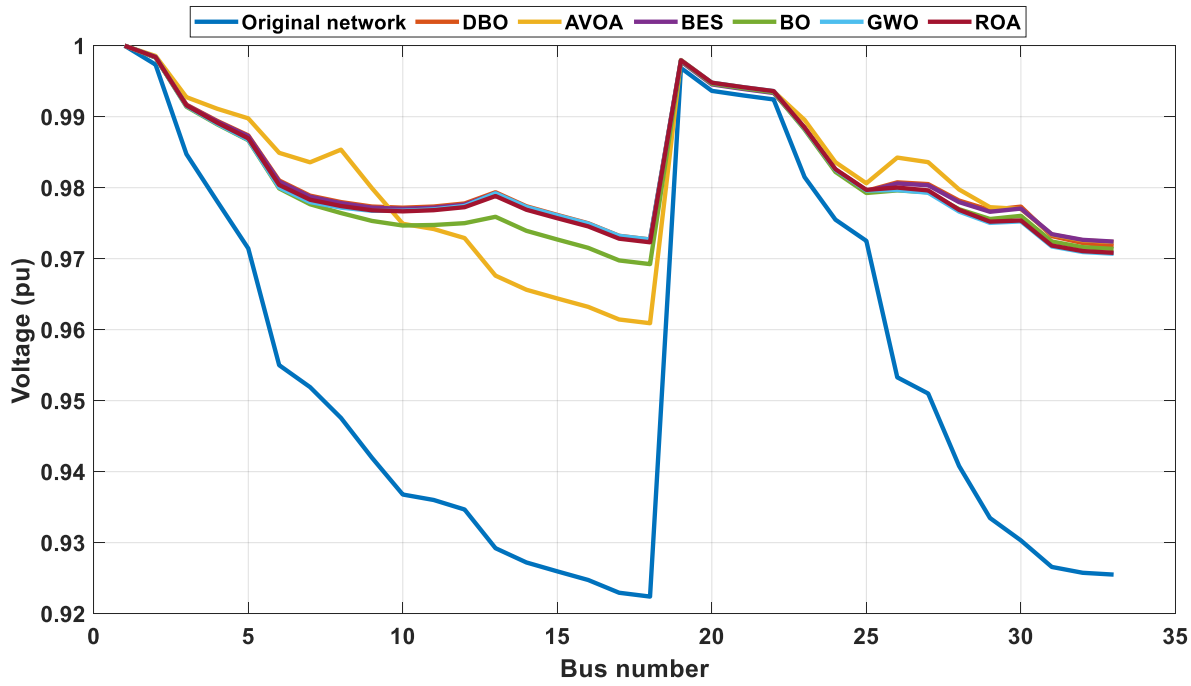

Figure 9. The network voltage profile throughout minimizing the first objective function of the IEEE-33 network.

The second fitness function minimized the voltage violation; the original network had a voltage violation of 36.477 pu. The fetched results in such case are given in Table 4, the proposed ROA accomplished the best voltage violation of 3.4762 pu, about a 90.47% enhancement of the original network, by installing RESs of 1499.994 kW and 1500 kW on buses 10 and 30, respectively, as well as 50 kW and 79.68228 kW FCSs on buses 2 and 10, respectively. This integration resulted in an active power loss of 1643.5811 kW. AVOA was the worst optimizer with a voltage deviation of 3.7866 pu. The voltage fluctuation versus number of iterations is shown in Figure 10, while the voltage patterns of the network

are displayed in Figure 11, the profile clarified significant improvement of the network voltages. The proposed ROA was the best optimizer compared to the others in achieving the least voltage deviation.

Table 4. The optimal results throughout minimizing the second objective function of the IEEE-33 bus network.

	DBO	AVOA	BES	BO	GWO	ROA
RES (kW)/location	1498.299/(10) 1500/(31)	1449.13/(11) 1500/(31)	1485.9678/(10) 1500/(30)	1500/(10) 1380.22/(31)	1500/(10) 1500(20)	1499.994/(10) 1500/(30)
FCS (kW)/location	50/(2) 181.6571/(33)	89.58208/(30) 82.92387/(33)	50/(33) 50/(26)	50/(2) 52.7957/(23)	74.7382/(10) 121.3876/(3)	50/(2) 79.68228/(10)
Active power loss (kW)	1838.1837	1748.6105	1743.0893	1840.8733	1654.1723	1643.5811
Reactive power loss (kVar)	1307.9386	1246.4018	1223.3889	1307.5806	1154.3989	1148.2444
Vmin (pu)/location	0.9833/(25)	0.9833/(25)	0.9837/(25)	0.9833/(25)	0.9828/(25)	0.9831/(25)
Vmax (pu)/location	1.0024/(10)	1.0026/(11)	1.0036/(10)	1.0025/(10)	1.0/(1)	1.0/(1)
Voltage deviation (pu)	3.7273	3.7866	3.5632	3.7378	3.5399	3.4762

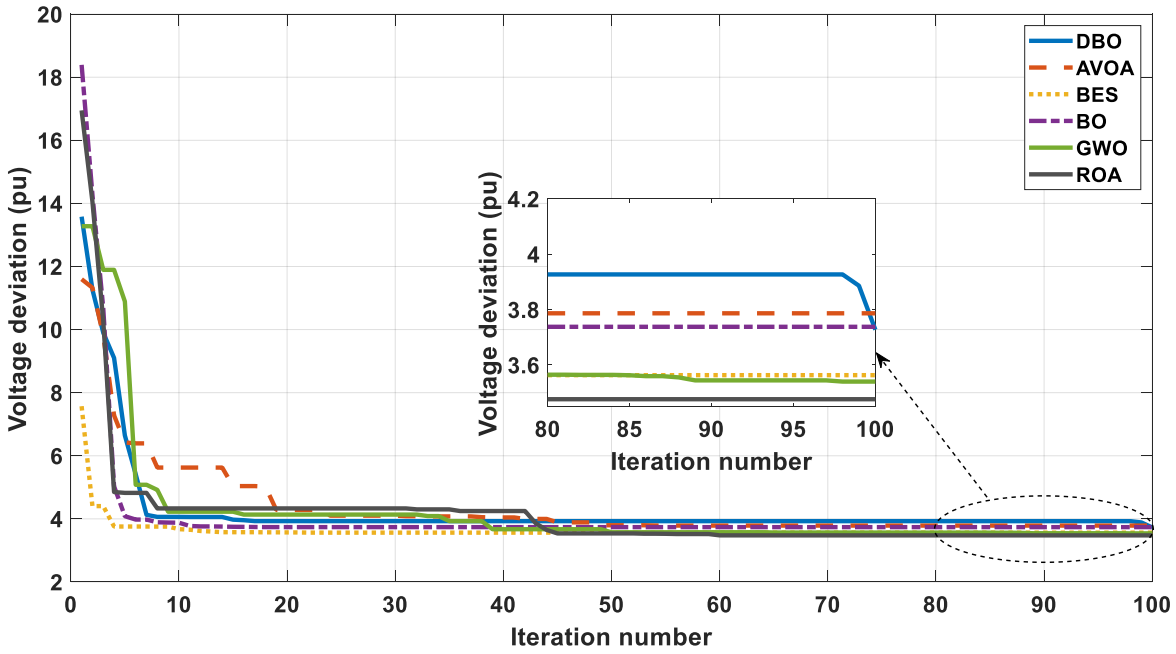

Figure 10. The voltage deviation versus the number of iterations throughout minimizing the second objective function of the IEEE-33 network.

The third case involved solving a multi-objective problem to minimize power loss and volage fluctuation; the proposed MOROA was compared to the multi-objective grey wolf optimizer (MOGWO), the multi-objective multi-verse optimizer (MOMVO), and the multi-objective artificial hummingbird algorithm (MOAHA) [47]. The optimal results are given in Table 5, RESs with 994.2378 kW and 1472.334 kW, and FCSs with 128.1094 kW and 165.3984 kW are recommended to be installed via the proposed MOROA on buses 13, 30, 2, and 30, respectively. This integration achieved active power loss and voltage violation of 1763.93 kW and 6.6547 pu, respectively, while MOAHA achieved the worst power loss and voltage violation of 1829.26 kW and 6.7704 pu, respectively. The results demonstrated the superiority of the proposed MOROA over the others. Moreover, the variations of both targets with number of iterations obtained via the proposed approach are given in Figure 12. Furthermore, the network voltage profiles before and after installing RESs and

FCSs are shown in Figure 13. The curves revealed that there is significant improvement in the network voltage profile.

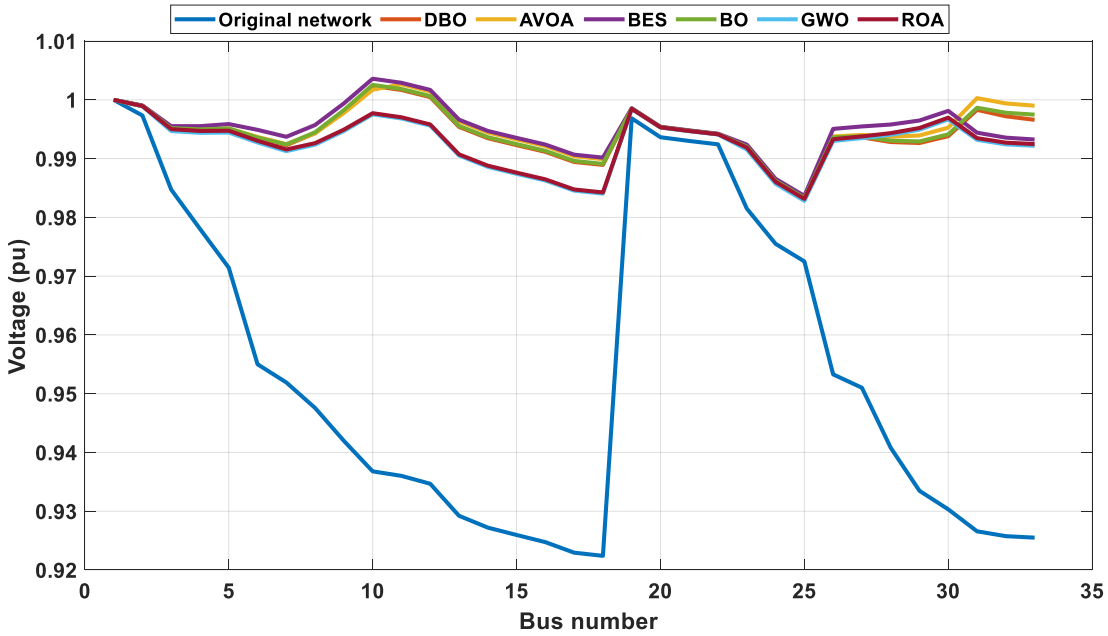

Figure 11. The network voltage profile throughout minimizing the second objective function of the IEEE-33 network.

Table 5. The optimal results throughout solving the multi-objective problem for the IEEE-33 bus network.

	MOAHA [47]	MOMVO	MOGWO	MOROA
RES (kW)/location	1475.0424/(30) 1073.4234/(15)	885.715/(14) 1465.69/(30)	1283.274/(11) 1264.667/(30)	994.2378/(13) 1472.334/(30)
FCS (kW)/location	63.763105/(14) 188.82647/(17)	51.3188/(3) 92.0779/(2)	190.1696/(2) 96.09850/(10)	128.1094/(2) 165.3984/(30)
Active power loss (kW)	1829.26	1810.31	1801.96	1763.93
Voltage deviation (pu)	6.7704	6.2317	6.4819	6.6547
Reactive power loss (kVar)	1152.29	1122.65	1108.20	1025.81
Vmin (pu)/location	0.9813/(25)	0.9813/(25)	0.9802/(18)	0.9798/(33)
Vmax (pu)/location	1.0/(1)	1.0/(1)	1.0/(1)	1.0/(1)

The obtained results confirmed the efficiency of ROA as it achieved the best fitness values for all scenarios investigated on the IEEE-33 bus network.

6.2. IEEE-69 Bus Network

The proposed ROA was also applied on the IEEE-69 bus system, it consisted of 68 branches and 69 nodes, the network nominal voltage was 12.66 kV and the base power was 100 MVA. The single line diagram of the IEEE-69 bus system is shown in Figure 14. The demand and branch data of the network were given in [53], the network is loaded by 24 h demand level given in Figure 7, the active power loss was 8665.356 kW whereas the reactive power loss was 3938.366 kVar. It was assumed that three renewable DGs were integrated in addition to three FCSs.

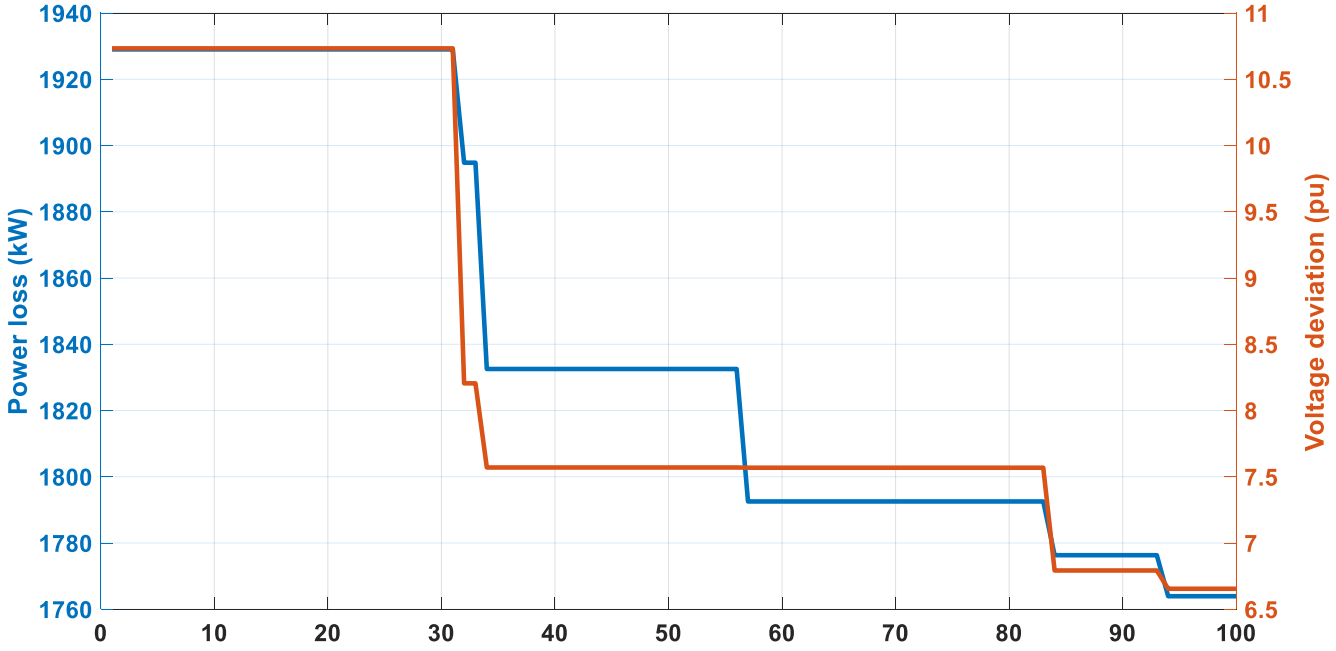

Figure 12. Variations of power loss and voltage violation throughout solving the multi-objective problem for the IEEE-33 network.

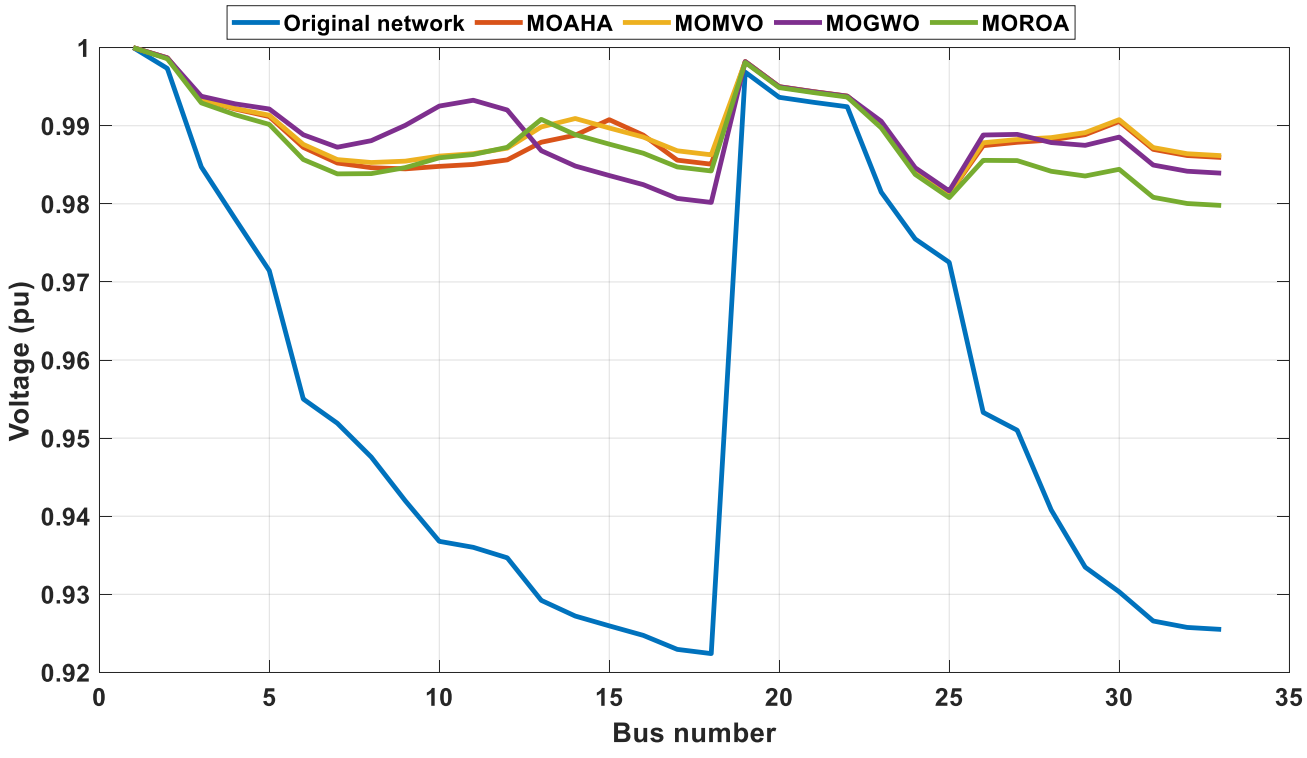

Figure 13. The network voltage profile throughout solving the multi-objective problem for the IEEE-33 network.

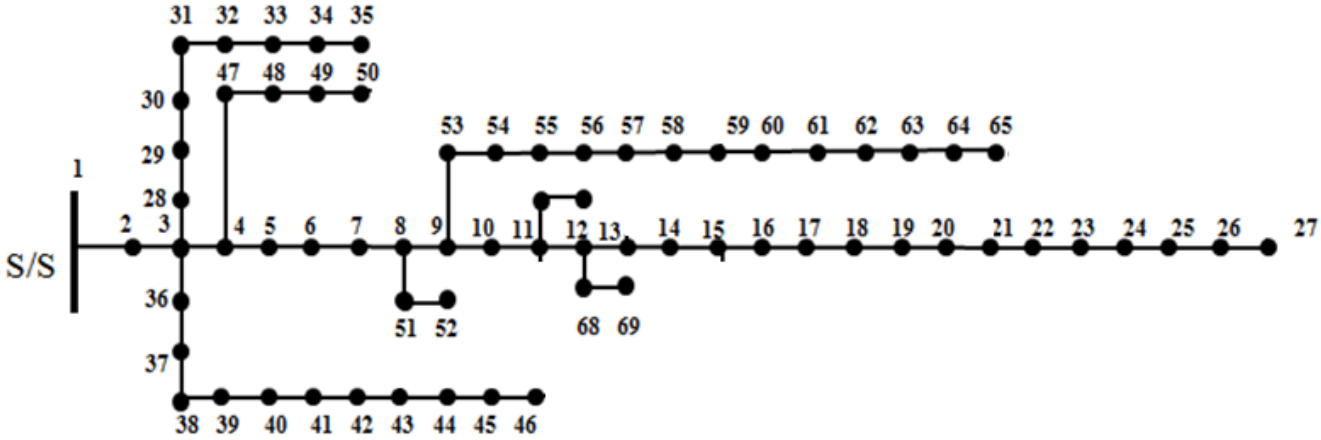

Figure 14. IEEE-69 bus network single line diagram.

The fetched results obtained by ROA and others throughout minimizing the network power loss are given in Table 6. The best loss was 2738.731 kW, achieved through the proposed ROA via installing RESs of 1500 kW, 663.715 kW, and 502.0473 kW on buses 61, 69, and 19, respectively, in addition to FCSs of 156.5290 kW, 50 kW, and 346.3399 kW on buses 19, 4, and 69, respectively. This integration reduced the active power loss by 68.39% compared to the original network. BO came in the second rank with a power loss of 2742.766 kW, while the worst one was 2905.728 kW, obtained by AVOA. Moreover, the proposed ROA required 62.078 s. to implement one run, this was the best obtained time. Figure 15 shows the variations of power losses during iterative process followed in each optimizer. Moreover, the voltage profile of the network is shown in Figure 16, it is clear that the voltage pattern is improved after integrating RESs and FCSs with sizes and sites obtained via the proposed ROA. The fetched results proved the superiority of ROA in minimizing the IEEE-69 bus system power losses.

Table 6. The optimal results throughout minimizing the first objective function of the IEEE-69 bus network.

	DBO	AVOA	BES	BO	GWO	ROA
RES (kW)/location	1500/(61) 518.641/(17) 54.7547/(14)	1500/(61) 295.224/(6) 813.401/(10)	713.821/(17) 584.281/(62) 1036.10/(61)	1500/(61) 426.56/(17) 485.21/(53)	1500/(61) 47.971/(23) 575.167/(12)	1500/(61) 663.715/(69) 502.0473/(19)
FCS (kW)/location	51.0967/(18) 50/(69) 50.6284/(5)	67.2109/(4) 53.2949/(51) 54.3663/(29)	58.7486/(18) 82.7298/(47) 191.153/(17)	50.019/(53) 50/(2) 50/(47)	64.7808/(35) 196.489/(47) 173.715/(29)	156.5290/(19) 50/(4) 346.3399/(69)
Active power loss (kW)	2810.358	2905.728	2775.538	2742.766	2819.619	2738.731
Reactive power loss (kVar)	1291.968	1311.428	1274.645	1259.164	1296.032	1276.838
Vmin (pu)/location	0.9796/(65)	0.9798/(27)	0.9836/(65)	0.9819/(65)	0.9804/(65)	0.9800/(65)
Vmax (pu)/location	1.0/(1)	1.0/(1)	1.0/(1)	1.0/(1)	1.0/(1)	1.0/(1)
Voltage deviation (pu)	11.4739	13.3273	11.5038	10.4405	13.3135	12.1014
Time (s)	159.893	104.103	347.468	62.493	145.821	62.078

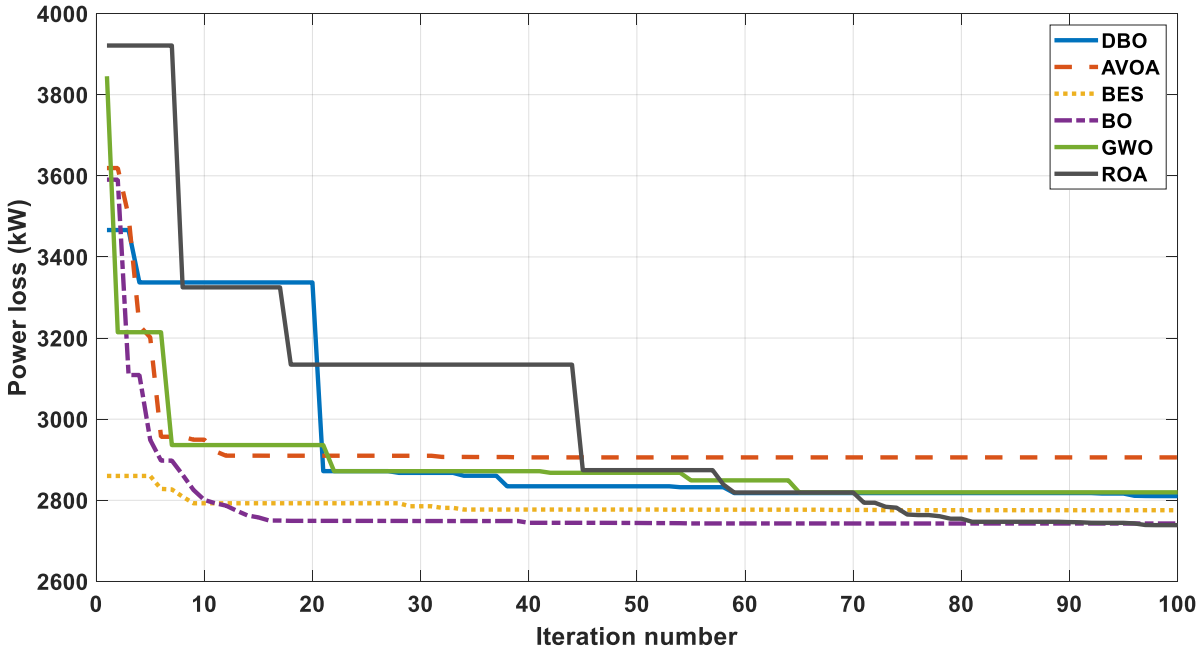

Figure 15. The power loss versus the number of iterations throughout minimizing the first objective function of the IEEE-69 network.

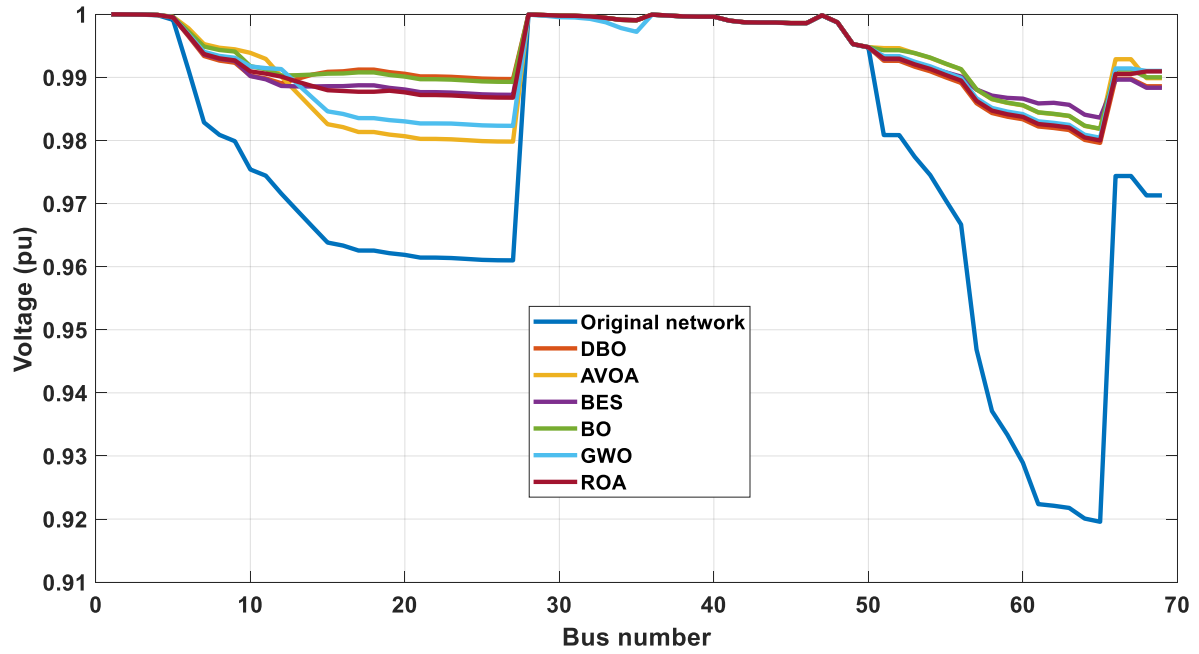

Figure 16. The network voltage profile throughout minimizing the first objective function of the IEEE-69 network.

The original network had a voltage violation of 39.229 pu; minimization of the voltage fluctuation was the second target, Table 7 tabulates the optimal fetched results in such case. The proposed ROA succeeded in mitigating the network voltage deviation to 2.6607 pu, about 93.22% enhancement of the original value, via installing RESs of 1464.69 kW, 1495.45 kW, and 891.503 kW on buses 63, 56, and 15, respectively, in addition to FCSs of 311.624 kW, 337.688 kW, and 231.826 kW on buses 7, 16, and 5, respectively. AVOA was still in the last rank, achieving a voltage deviation of 4.2701 pu. The performances of the optimizers considered are given in Figure 17, while the voltage patterns with/without the

installed DGs and stations are given in Figure 18. The results demonstrated the excellence of the proposed method while reducing the voltage fluctuation of the IEEE-69 bus network.

Table 7. The optimal results throughout minimizing the second objective function of the IEEE-69 bus network.

	DBO	AVOA	BES	BO	GWO	ROA
RES (kW)/location	987.669/(63) 1152.20/(13) 1416.90/(63)	1500/(12) 1500/(64) 607.458/(54)	1499.996/(63) 1499.999/(68) 469.3114/(58)	801.0936/(64) 1500/(59) 1500/(69)	549.582/(19) 1500/(62) 1500/(55)	1464.69/(63) 1495.45/(56) 891.503/(15)
FCS (kW)/location	245.784/(43) 253.716/(64) 308.648/(56)	350/(7) 234.083/(46) 333.914/(31)	53.66301/(58) 50/(2) 163.3407/(67)	50/(36) 350/(58) 192.210/(66)	162.323/(29) 58.5327/(21) 149.570/(47)	311.624/(7) 337.688/(16) 231.826/(5)
Active power loss (kW)	3316.866	3518.4419	3534.8244	3636.6704	3176.7778	3284.3169
Reactive power loss (kVar)	1626.321	1740.1091	1659.1212	1696.3122	1602.5207	1645.6244
Vmin (pu)/location	0.9941/(56)	0.9870/(61)	0.9912/(65)	0.9922/(61)	0.9903/(65)	0.9915/(65)
Vmax (pu)/location	1.0040/(13)	1.0055/(12)	1.0096/(68)	1.0100/(69)	1.0024/(55)	1.0021/(56)
Voltage deviation (pu)	3.748	4.2701	3.4861	3.5533	2.7751	2.6607

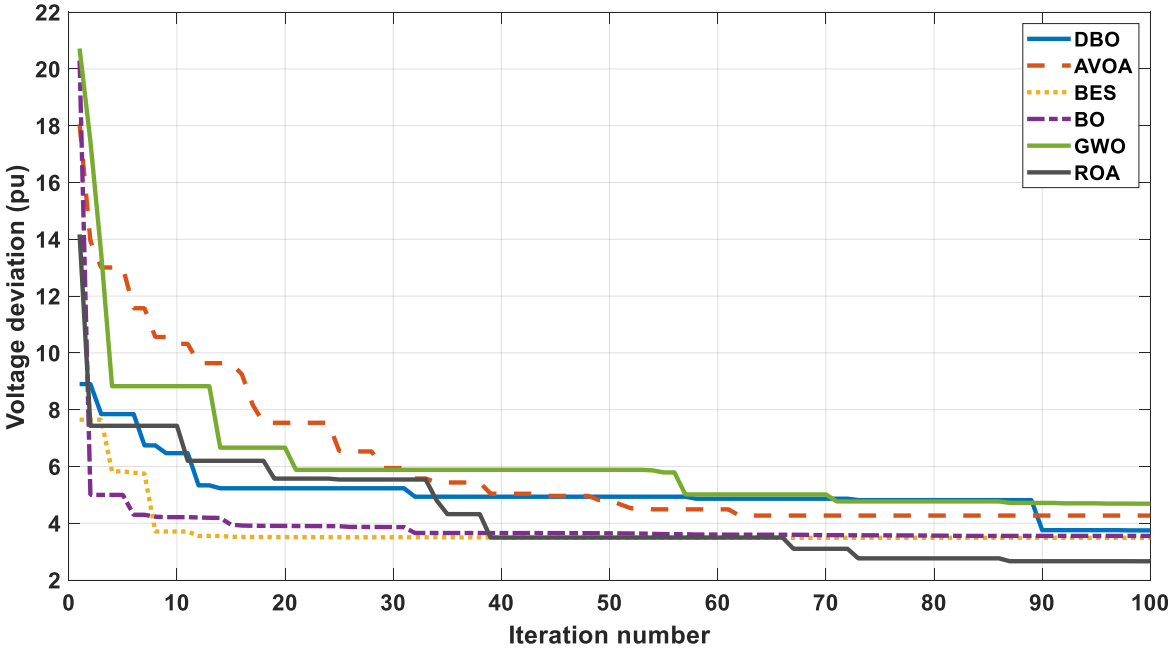

Figure 17. Voltage deviation variation throughout minimizing the second objective function of the IEEE-69 network.

Finally, the multi-objective problem for the IEEE-69 bus network was solved via the proposed MOROA in comparison to others, the fetched results are tabulated in Table 8. The best power loss and voltage violation were 2929.075 kW and 4.3347 pu, respectively, obtained via the proposed algorithm. The MOGWO achieved the worst power loss with a value of 3351.509 kW, whereas the largest voltage deviation was 6.832 pu, obtained via MOMVO. Also, the power loss and voltage fluctuation versus the number of iterations are shown in Figure 19, while the network voltage patterns are shown in Figure 20. The proposed approach proved its preference in finding the best locations and sizes of RESs and charging stations while solving the multi-objective problem.

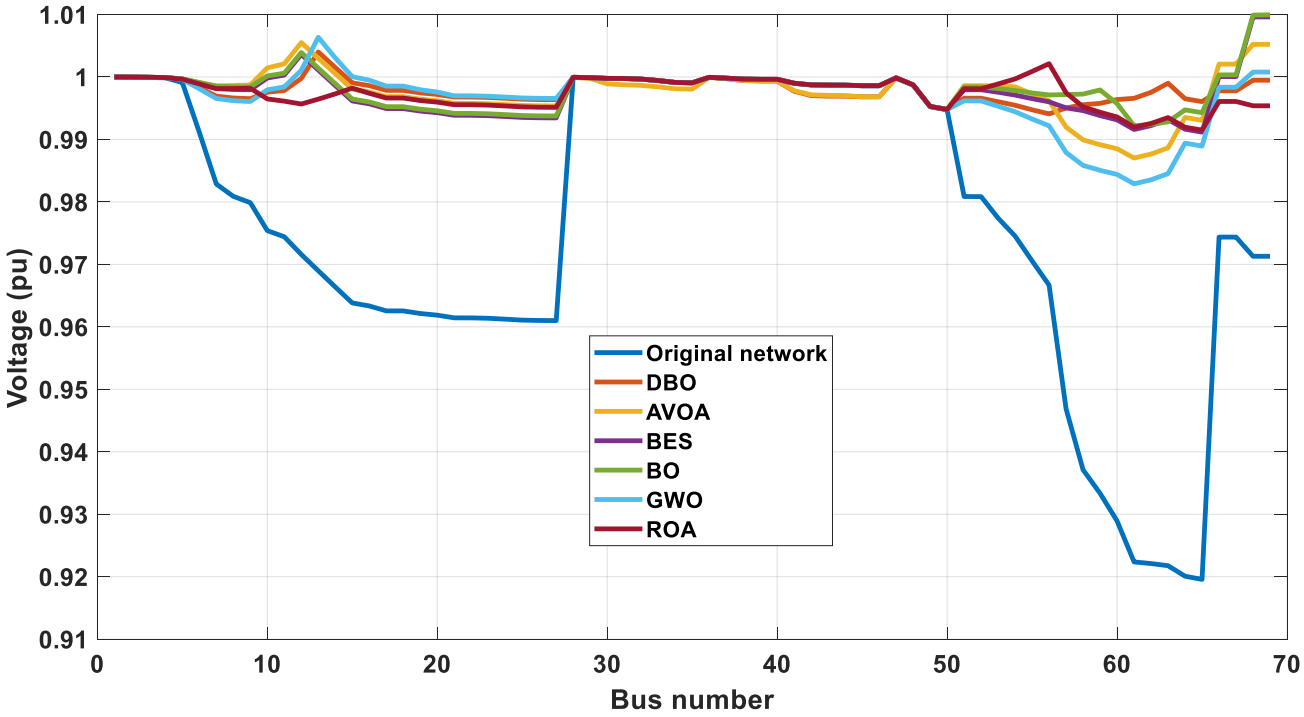

Figure 18. The network voltage profile throughout minimizing the second objective function of the IEEE-69 network.

Table 8. The optimal results throughout solving the multi-objective problem for the IEEE-69 bus network.

	MOAHA [47]	MOMVO	MOGWO	MOROA
RES (kW)/location	1469.52/(61) 916.516/(18) 301.015/(59)	1249.069/(49) 1500/(61) 855.449/(14)	1260.96/(68) 1395.23/(51) 1470.41/(62)	917.811/(9) 647.6445/(15) 1500/(61)
FCS (kW)/location	307.607/(47) 60.7376/(52) 207.741/(26)	98.1616/(34) 80.8805/(43) 207.898/(31)	305.866/(68) 307.682/(6) 296.051/(51)	248.222/(28) 135.164/(2) 336.811/(37)
Active power loss (kW)	2974.105	2960.5889	3351.509	2929.075
Voltage deviation (pu)	5.1243	6.832	5.4632	4.3347
Reactive power loss (kVar)	1294.045	1232.638	1501.993	1303.072
Vmin (pu)/location	0.9881/(65)	0.9817/(65)	0.9812/(65)	0.9856/(65)
Vmax (pu)/location	1.0002/(18)	1.0/(1)	1.0008/(68)	1.0005/(15)

A new methodology incorporating the ROA is proposed to find the best locations and capacities of RESs and FCSs in distribution systems. Power loss and voltage fluctuation are the considered targets to be minimized. Both single objective and multi-objective problems are formulated and solved via the proposed ROA. The power loss and voltage deviation of the IEEE-33 bus were reduced by 58.24% and 90.47%, respectively, with the aid of the proposed ROA. While benefits of 68.39% for losses and 93.22% for voltage deviation were achieved for the IEEE-69 bus network. Finally, the proposed ROA can be recommended as an effective tool to solve the problem of integrating RESs and EV FCSs in a radial distribution network.

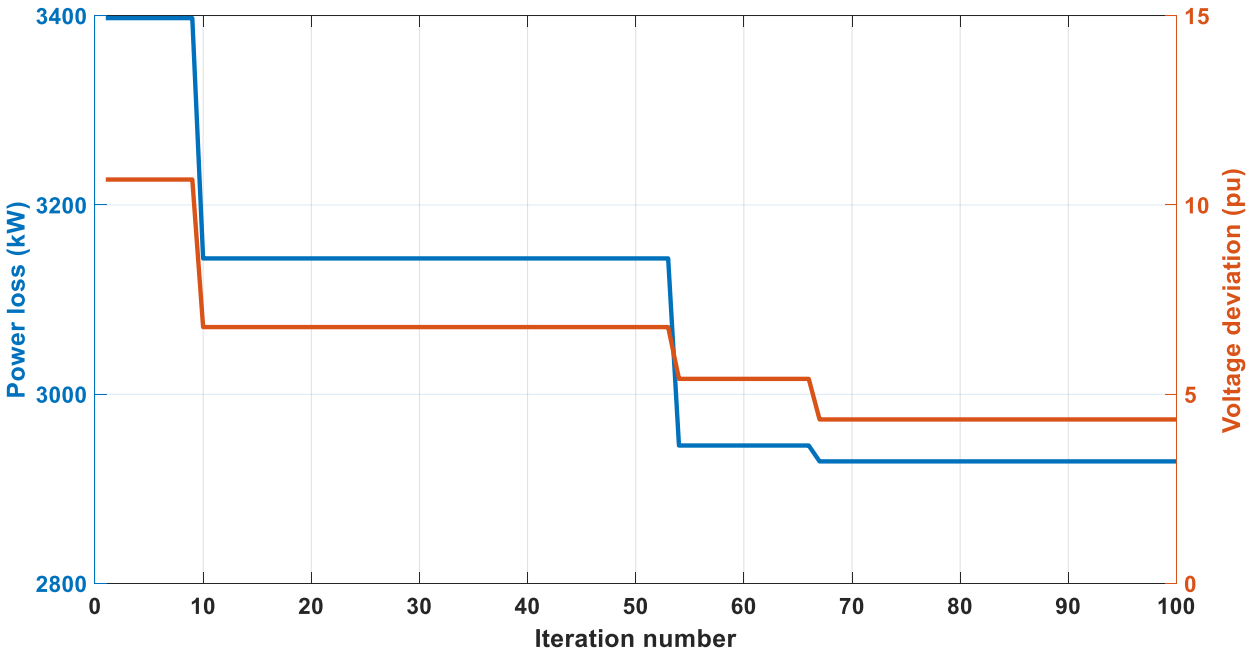

Figure 19. Variations of power loss and voltage violation throughout solving the multi-objective problem for the IEEE-69 network.

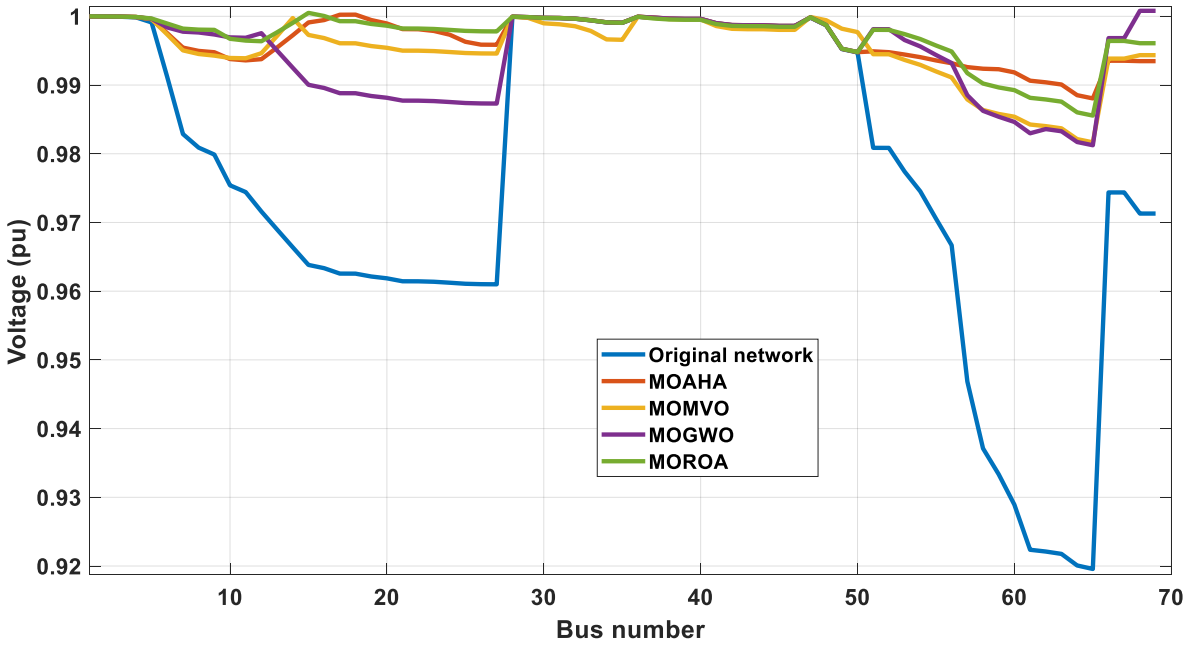

Figure 20. The network voltage profile throughout solving the multi-objective problem for the IEEE-69 network.

7. Conclusions

This paper proposed a new metaheuristic approach of the red kite optimization algorithm (ROA) to identify the best sites and sizes of RESs and FCSs in distribution networks. The ROA was selected due to its simplicity, requirement of less controlling parameters, high convergence rate, and balance between exploration and exploitation phases that enabled the algorithm to escape from local optima. The targets were minimizing the network active power loss and voltage fluctuation. Also, a multi-objective red kite optimization algorithm (MOROA) was proposed to mitigate both targets. Two standard

radial distribution networks, the IEEE-33 bus and the IEEE-69 bus, were analyzed. In the first network, two RESs and two FCSs were installed while in the second network three RESs and three FCSs were integrated. Comparisons to DBO, AVOA, BES, BO, and GWO in the single objective problem in addition to MOGWO, MOMVO, and MOAHA in the multi-objective problem were conducted. The proposed ROA gave the best solution in the IEEE-33 bus, reducing the network loss and voltage violation by 58.24% and 90.47%, respectively, whereas it achieved benefits of 68.39% for losses and 93.22% for voltage deviation of the IEEE-69 bus network. The obtained results revealed the robustness and competence of the proposed ROA in achieving the best results. Minimizing the period of charging for EVs will be considered as the target in future works. Also, the investigation of a real distribution network will be conducted in the next works.

Author Contributions: Conceptualization, S.M.A. and A.F.; methodology, A.F.; software, A.F.; validation, S.M.A. and A.F.; formal analysis, S.M.A.; investigation, A.F.; resources, A.F.; data curation, S.M.A.; writing—original draft preparation, A.F.; writing—review and editing, S.M.A.; visualization, S.M.A.; supervision, S.M.A.; project administration, A.F.; funding acquisition, S.M.A. All authors have read and agreed to the published version of the manuscript.

Funding: The authors extend their appreciation to the Deputyship for Research & Innovation, Ministry of Education in Saudi Arabia for funding this research through project number 223202.

Data Availability Statement: Not applicable.

Conflicts of Interest: The authors declare no conflict of interest.

References

1. Fazelpour, F.; Vafaeipour, M.; Rahbari, O.; Rosen, M.A. Intelligent optimization to integrate a plug-in hybrid electric vehicle smart parking lot with renewable energy resources and enhance grid characteristics. *Energy Convers. Manag.* **2014**, *77*, 250–261. [CrossRef]
2. Amini, M.H.; Boroojeni, K.G.; Wang, C.J.; Nejadpak, A.; Iyengar, S.S.; Karabasoglu, O. Effect of electric vehicle parking lots' charging demand as dispatchable loads on power systems loss. In Proceedings of the 2016 IEEE International Conference on Electro Information Technology (EIT), Grand Forks, ND, USA, 19–21 May 2016; pp. 499–503. [CrossRef]
3. Xu, N.Z.; Chung, C.Y. Uncertainties of EV charging and effects on well-being analysis of generating systems. *IEEE Trans. Power Syst.* **2014**, *30*, 2547–2557. [CrossRef]
4. Kumar, Y.V.P.; Rao, S.N.V.B.; Padma, K.; Reddy, C.P.; Pradeep, D.J.; Flah, A.; Kraiem, H.; Jasiński, M.; Nikolovski, S. Fuzzy hysteresis current controller for power quality enhancement in renewable energy integrated clusters. *Sustainability* **2022**, *14*, 4851. [CrossRef]
5. Rao, S.B.; Kumar, Y.P.; Amir, M.; Ahmad, F. An adaptive neuro-fuzzy control strategy for improved power quality in multi-microgrid clusters. *IEEE Access* **2022**, *10*, 128007–128021. [CrossRef]
6. Amer, A.; Azzouz, M.A.; Azab, A.; Awad, A.S. Stochastic planning for optimal allocation of fast charging stations and wind-based DGs. *IEEE Syst. J.* **2020**, *15*, 4589–4599. [CrossRef]
7. Sachan, S.; Amini, M.H. Optimal allocation of EV charging spots along with capacitors in smart distribution network for congestion management. *Int. Trans. Electr. Energy Syst.* **2020**, *30*, 12507. [CrossRef]
8. Mohanty, A.K.; Suresh Babu, P.; Salkuti, S.R. Optimal allocation of fast charging station for integrated electric-transportation system using multi-objective approach. *Sustainability* **2022**, *14*, 14731. [CrossRef]
9. Zeng, B.; Zhu, Z.; Xu, H.; Dong, H. Optimal public parking lot allocation and management for efficient PEV accommodation in distribution systems. *IEEE Trans. Ind. Appl.* **2020**, *56*, 5984–5994. [CrossRef]
10. Gupta, R.S.; Tyagi, A.; Anand, S. Optimal allocation of electric vehicles charging infrastructure, policies and future trends. *J. Energy Storage* **2021**, *43*, 103291. [CrossRef]
11. Kong, W.; Luo, Y.; Feng, G.; Li, K.; Peng, H. Optimal location planning method of fast charging station for electric vehicles considering operators, drivers, vehicles, traffic flow and power grid. *Energy* **2019**, *186*, 115826. [CrossRef]
12. Battapothula, G.; Yammani, C.; Maheswarapu, S. Multi-objective simultaneous optimal planning of electrical vehicle fast charging stations and DGs in distribution system. *J. Mod. Power Syst. Clean Energy* **2019**, *7*, 923–934. [CrossRef]
13. Khan, W.; Ahmad, F.; Alam, M.S. Fast EV charging station integration with grid ensuring optimal and quality power exchange. *Eng. Sci. Technol. Int. J.* **2019**, *22*, 143–152. [CrossRef]
14. Pal, A.; Bhattacharya, A.; Chakraborty, A.K. Placement of public fast-charging station and solar distributed generation with battery energy storage in distribution network considering uncertainties and traffic congestion. *J. Energy Storage* **2021**, *41*, 102939. [CrossRef]

15. Wu, X.; Feng, Q.; Bai, C.; Lai, C.S.; Jia, Y.; Lai, L.L. A novel fast-charging stations locational planning model for electric bus transit system. *Energy* **2021**, *224*, 120106. [CrossRef]
16. Sa'adati, R.; Jafari-Nokandi, M.; Saebi, J. Allocation of RESs and PEV fast-charging station on coupled transportation and distribution networks. *Sustain. Cities Soc.* **2021**, *65*, 102527. [CrossRef]
17. Amer, A.; Azab, A.; Azzouz, M.A.; Awad, A.S. A stochastic program for siting and sizing fast charging stations and small wind turbines in urban areas. *IEEE Trans. Sustain. Energy* **2021**, *12*, 1217–1228. [CrossRef]
18. Pal, A.; Bhattacharya, A.; Chakraborty, A.K. Allocation of electric vehicle charging station considering uncertainties. *Sustain. Energy Grids Netw.* **2021**, *25*, 100422. [CrossRef]
19. Rajesh, P.; Shajin, F.H. Optimal allocation of EV charging spots and capacitors in distribution network improving voltage and power loss by Quantum-Behaved and Gaussian Mutational Dragonfly Algorithm (QGDA). *Electr. Power Syst. Res.* **2021**, *194*, 107049. [CrossRef]
20. Narasipuram, R.P.; Mopidevi, S. A technological overview & design considerations for developing electric vehicle charging stations. *J. Energy Storage* **2021**, *43*, 103225. [CrossRef]
21. Ahmad, F.; Khalid, M.; Panigrahi, B.K. An enhanced approach to optimally place the solar powered electric vehicle charging station in distribution network. *J. Energy Storage* **2021**, *42*, 103090. [CrossRef]
22. Deb, S.; Gao, X.Z.; Tammi, K.; Kalita, K.; Mahanta, P. A novel chicken swarm and teaching learning based algorithm for electric vehicle charging station placement problem. *Energy* **2021**, *220*, 119645. [CrossRef]
23. Goswami, A.; Sadhu, P.K. Stochastic firefly algorithm enabled fast charging of solar hybrid electric vehicles. *Ain Shams Eng. J.* **2021**, *12*, 529–539. [CrossRef]
24. Khaksari, A.; Tsaousoglou, G.; Makris, P.; Steriotis, K.; Efthymiopoulos, N.; Varvarigos, E. Sizing of electric vehicle charging stations with smart charging capabilities and quality of service requirements. *Sustain. Cities Soc.* **2021**, *70*, 102872. [CrossRef]
25. Bhadoriya, J.S.; Gupta, A.R.; Zellagui, M.; Saxena, N.K.; Arya, A.K.; Bohre, A.K. Optimal allocation of electric vehicles charging station in distribution network beside DG using TSO. In *Planning of Hybrid Renewable Energy Systems, Electric Vehicles and Microgrid: Modeling, Control and Optimization*; Springer Nature: Singapore, 2022; pp. 785–808. [CrossRef]
26. Yi, T.; Cheng, X.; Peng, P. Two-stage optimal allocation of charging stations based on spatiotemporal complementarity and demand response: A framework based on MCS and DBPSO. *Energy* **2022**, *239*, 122261. [CrossRef]
27. Ghasemi-Marzbali, A. Fast-charging station for electric vehicles, challenges and issues: A comprehensive review. *J. Energy Storage* **2022**, *49*, 104136. [CrossRef]
28. Zhou, G.; Zhu, Z.; Luo, S. Location optimization of electric vehicle charging stations: Based on cost model and genetic algorithm. *Energy* **2022**, *247*, 123437. [CrossRef]
29. Aljehane, N.O.; Mansour, R.F. Optimal allocation of renewable energy source and charging station for PHEVs. *Sustain. Energy Technol. Assess.* **2022**, *49*, 101669. [CrossRef]
30. Ahmad, F.; Iqbal, A.; Ashraf, I.; Marzband, M. Optimal location of electric vehicle charging station and its impact on distribution network: A review. *Energy Rep.* **2022**, *8*, 2314–2333. [CrossRef]
31. Kumar, N.; Kumar, T.; Nema, S.; Thakur, T. A comprehensive planning framework for electric vehicles fast charging station assisted by solar and battery based on Queueing theory and non-dominated sorting genetic algorithm-II in a co-ordinated transportation and power network. *J. Energy Storage* **2022**, *49*, 104180. [CrossRef]
32. Zu, S.; Sun, L. Research on location planning of urban charging stations and battery-swapping stations for electric vehicles. *Energy Rep.* **2022**, *8*, 508–522. [CrossRef]
33. Thangaraju, I. Optimal allocation of distributed generation and electric vehicle charging stations-based SPOA2B approach. *Int. J. Intell. Syst.* **2022**, *37*, 2061–2088. [CrossRef]
34. Al Wahedi, A.; Bicer, Y. Techno-economic optimization of novel stand-alone renewables-based electric vehicle charging stations in Qatar. *Energy* **2022**, *243*, 123008. [CrossRef]
35. Deb, S.; Gao, X.Z.; Tammi, K.; Kalita, K.; Mahanta, P. Nature-inspired optimization algorithms applied for solving charging station placement problem: Overview and comparison. *Arch. Comput. Methods Eng.* **2021**, *28*, 91–106. [CrossRef]
36. Erdogan, N.; Pamucar, D.; Kucuksari, S.; Deveci, M. An integrated multi-objective optimization and multi-criteria decision-making model for optimal planning of workplace charging stations. *Appl. Energy* **2021**, *304*, 117866. [CrossRef]
37. Ma, T.Y.; Xie, S. Optimal fast charging station locations for electric ridesharing with vehicle-charging station assignment. *Transp. Res. Part D Transp. Environ.* **2021**, *90*, 102682. [CrossRef]
38. Ahmadi, M.; Hosseini, S.H.; Farsadi, M. Optimal allocation of electric vehicles parking lots and optimal charging and discharging scheduling using hybrid metaheuristic algorithms. *J. Electr. Eng. Technol.* **2021**, *16*, 759–770. [CrossRef]
39. Fathy, A.; Abdelaziz, A.Y. Competition over resource optimization algorithm for optimal allocating and sizing parking lots in radial distribution network. *J. Clean. Prod.* **2020**, *264*, 121397. [CrossRef]
40. Khan, M.J.; Iqbal, M.T. Pre-feasibility study of stand-alone hybrid energy systems for applications in Newfoundland. *Renew. Energy* **2005**, *30*, 835–854. [CrossRef]
41. Moghaddam, A.A.; Seifi, A.; Niknam, T. Multi-operation management of a typical micro-grids using Particle Swarm Optimization: A comparative study. *Renew. Sustain. Energy Rev.* **2012**, *16*, 1268–1281. [CrossRef]
42. Fathy, A.; Kaaniche, K.; Alanazi, T.M. Recent approach based social spider optimizer for optimal sizing of hybrid PV/wind/battery/diesel integrated microgrid in aljouf region. *IEEE Access* **2020**, *8*, 57630–57645. [CrossRef]

43. Roe, C.; Meliopoulos, A.P.; Meisel, J.; Overbye, T. November. Power system level impacts of plug-in hybrid electric vehicles using simulation data. In Proceedings of the 2008 IEEE Energy 2030 Conference, Atlanta, GA, USA, 17–18 November 2008; pp. 1–6. [CrossRef]
44. Mozafar, M.R.; Moradi, M.H.; Amini, M.H. A simultaneous approach for optimal allocation of renewable energy sources and electric vehicle charging stations in smart grids based on improved GA-PSO algorithm. *Sustain. Cities Soc.* **2017**, *32*, 627–637. [CrossRef]
45. Li, Z.; Chowdhury, M.; Bhavsar, P.; He, Y. Optimizing the performance of vehicle-to-grid (V2G) enabled battery electric vehicles through a smart charge scheduling model. *Int. J. Automot. Technol.* **2015**, *16*, 827–837. [CrossRef]
46. Gahruei, J.R.; Beheshti, Z. The Electricity Consumption Prediction using Hybrid Red kite Optimization Algorithm with Multi-Layer Perceptron Neural Network. *J. Intell. Proced. Electr. Technol.* **2022**, *15*, 1–22.
47. Fathy, A. A novel artificial hummingbird algorithm for integrating renewable based biomass distributed generators in radial distribution systems. *Appl. Energy* **2022**, *323*, 119605. [CrossRef]
48. Xue, J.; Shen, B. Dung beetle optimizer: A new meta-heuristic algorithm for global optimization. *J. Supercomput.* **2023**, *79*, 7305–7336. [CrossRef]
49. Abdollahzadeh, B.; Gharehchopogh, F.S.; Mirjalili, S. African vultures optimization algorithm: A new nature-inspired metaheuristic algorithm for global optimization problems. *Comput. Ind. Eng.* **2021**, *158*, 107408. [CrossRef]
50. Alsattar, H.A.; Zaidan, A.A.; Zaidan, B.B. Novel meta-heuristic bald eagle search optimisation algorithm. *Artif. Intell. Rev.* **2020**, *53*, 2237–2264. [CrossRef]
51. Das, A.K.; Pratihar, D.K. Bonobo optimizer (BO): An intelligent heuristic with self-adjusting parameters over continuous spaces and its applications to engineering problems. *Appl. Intell.* **2022**, *52*, 2942–2974. [CrossRef]
52. Mirjalili, S.; Mirjalili, S.M.; Lewis, A. Grey wolf optimizer. *Adv. Eng. Softw.* **2014**, *69*, 46–61. [CrossRef]
53. Fathy, A.; Abdelaziz, A.Y. Grey wolf optimizer for optimal sizing and siting of energy storage system in electric distribution network. *Electr. Power Compon. Syst.* **2017**, *45*, 601–614. [CrossRef]